The 2006 Eruption of Augustine Volcano, Alaska
Power, J.A., Coombs, M.L., and Freymueller, J.T., editors
U.S. Geological Survey Professional Paper 1769

Chapter 3

Using Seismic *b*-Values to Interpret Seismicity Rates and Physical Processes During the Preeruptive Earthquake Swarm at Augustine Volcano 2005–2006

By Katrina M. Jacobs[1] and Stephen R. McNutt[2]

Abstract

We use seismic *b*-values to explore physical processes during the Augustine Volcano 2005–6 preeruptive earthquake swarm. The preeruptive earthquake swarm was divided into two parts: the "long swarm," which extended from April 30, 2005, to January 10, 2006; and the "short swarm," which started 13 hours before the onset of explosive activity on January 11, 2006. Calculations of *b*-value for each of these swarms and for a background period were performed. The short swarm, directly preceding the eruption, had the lowest calculated *b*-value. In addition to the low value, the shape of the *b*-value plot for the short swarm appears to have two separate slopes, a shallower slope for magnitudes as great as 1.2 and a steeper slope for magnitudes greater than 1.2. Calculations of *b* were also run for three precursory deformation stages suggested by a separate investigation of deformation at Augustine Volcano. The highest *b*-value, found in stage 2, may indicate an increase in pore pressure and in thermal gradient, which matches the geodetic interpretation of a proposed dike intrusion. Finer resolution changes of *b* are explored through calculations of *b*-value versus time. An initial drop in *b*-value in late 2004 preceded the onset of increased seismicity. The temporal nature of this change and its timing are corroborated by atmospheric temperature data recorded on the summit of the volcano, which increased at approximately the same time. Stress at Augustine Volcano was also studied using 79 earthquakes that returned acceptable focal mechanisms between January 1, 2002, and January 10, 2006. These mechanisms and an attempted stress-tensor inversion imply that stresses within the Augustine edifice are highly variable and do not display a dominant faulting style. A population of high-frequency volcano-tectonic earthquakes during the short swarm is found to have accompanying very-long-period (20 seconds and greater) energy. Statistical analysis indicates that these earthquakes are a separate population of events. We interpret this population of earthquakes to represent a separate and distinct physical process that was not seen before the 13 hours preceding the eruption. The *b*-value time series also indicates that when changes in stress, pore pressure, and thermal gradient occur simultaneously, that stress effects dominate the observed *b*-value.

Introduction

The 2006 eruption of Augustine Volcano was preceded by 8 months of increased rates of volcano-tectonic (VT) earthquakes, similarly to previous eruptions in 1976 and 1986 (Power and Lalla, this volume). The eruption lasted from January 11 through mid-March, 2006, and was characterized by explosions, effusive activity, and pyroclastic flows. Only earthquakes that occurred before the onset of explosive activity on January 11 are examined here in hopes that we can gain insight about the sequence of processes that led up to the 2006 eruption. Study of this preeruptive period may provide better information for those monitoring future earthquake swarms at Augustine and other similar volcanoes. Although this study will focus on the earthquakes that occurred during the preeruptive earthquake swarm (April 30, 2005 to January 10, 2006), we also use Alaska Volcano Observatory (AVO) catalog data beginning in the year 2000 to establish background rates and a start date for the precursory swarm. A histogram showing

[1] School of Geography, Environment and Earth Sciences, Victoria University of Wellington, P.O. Box 600, Wellington, New Zealand.

[2] Alaska Volcano Observatory, University of Alaska Fairbanks Geophysical Institute, 903 Koyukuk Dr., Fairbanks, AK 99775.

located earthquakes per 30 days from January 1, 2000, through the January 11, 2006, eruptive activity can be seen in figure 1.

The concept of seismic *b*-values was first put forward by Ishimoto and Ida (1939) and was later recast in its more familiar form as the value of *b* in the Gutenberg and Richter relation, $\log N = a - bM$, where "*N*" is the cumulative number of events greater than or equal to magnitude "*M*", and "a" is an empirical constant (Ishimoto and Ida, 1939; Gutenberg and Richter, 1944). The *b*-value can also be thought of as a ratio of the number of small earthquakes to the number of larger earthquakes happening over a given period of time. Seismic *b*-values are often near one for tectonic areas and are found to be higher in volcanic areas (Bath, 1981; McNutt, 2005).

Seismic *b*-values have been shown to vary with several known physical parameters, including stress (Scholz, 1968), thermal gradient (Warren and Latham, 1970), pore pressure (Wyss, 1973), and fracture density (material heterogeneity) (Mogi, 1962). These physical parameters are likely to be affected by a variety of processes which are common at volcanoes. Given the links to these physical changes, investigating *b*-values has the potential to determine physical processes that are driving earthquake swarms.

Although *b*-values have been found to vary with four physical parameters, only three are considered here; material heterogeneity has been excluded from this study. Both Scholz (1968) and Warren and Latham (1970) suggest that some *b*-value changes initially thought to be due to material heterogeneity are in fact caused by stress differences or thermal gradient changes. Heterogeneity is often attributed to fixed rock properties, such as porosity or fracture density, and though it may vary slightly because of ongoing fracture formation and deformation, it is more likely to vary on long geologic time scales rather than short eruptive time scales (Zobin, 1979). Additionally, factors that make the material more heterogeneous, such as new fractures and injection of a magma body (fluid next to rock), are likely to produce transient signatures in the other three physical parameters.

Many *b*-values studies have been conducted at volcanoes. These investigations have covered both spatial mapping of *b*-values and temporal analyses. Spatial studies have identified small volumes of high *b*-values that have been interpreted as magma bodies (Wiemer and McNutt, 1997; Wiemer and others, 1998; Sanchez and others, 2004). At Long Valley caldera and at Martin and Mageik volcanoes significant temporal changes in *b*-value were observed during earthquake swarms (Wiemer and others, 1998; Jolly and McNutt, 1999). The small seismic volume at Augustine (fig. 2) makes it an ideal candidate for a temporal *b*-value study.

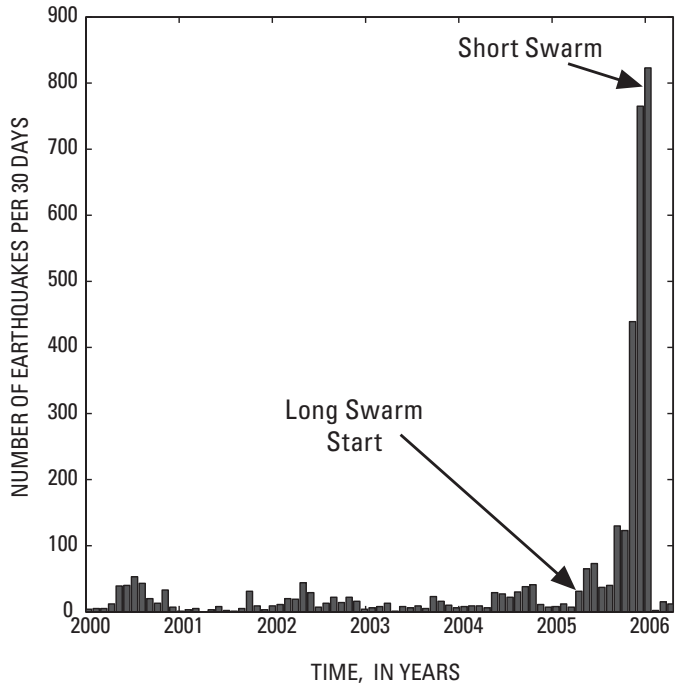

Figure 1. Histogram for located earthquakes per 30 days at Augustine Volcano from January 1, 2000, to January 11, 2006. Arrows point to the bins containing the start date of the long swarm (April 30, 2005) and the short swarm (January 10–11, 2006). Tick marks on the horizontal axis mark the beginning of each year.

Data

All located earthquakes at Augustine Volcano from 2000 through 2006 were selected from the AVO catalog. AVO maintains an earthquake catalog and publishes annual reports (for example, Dixon and others, 2008). The selected Augustine earthquake catalog has 2,945 located earthquakes between January 1, 2000, and the onset of the 2006 eruption on January 11, 2006. More than half (2,005) of the earthquakes are associated with the 2005–2006 preeruptive earthquake swarm. A rate histogram for the Augustine activity is shown in figure 1. Augustine earthquakes are located with an on-island seismic network that consists of 8 telemetered stations with 15 components (Dixon and others, 2008). Figure 2 shows a map of the island, its seismic instrumentation, and plots of the earthquake hypocenters selected from the AVO catalog. AVO catalog locations are determined using a one-dimensional six-layer velocity model derived from the model described by Lalla and Power (this volume). Processing is done using the XPICK seismic analysis software (Robinson, 1990) and the earthquake location program HYPOELLIPSE (Lahr, 1999). Magnitudes of completeness for Augustine Volcano ranged from 0.1 to -0.2 in 2005 (Dixon and others, 2008).

To use *b*-values to investigate temporal variations in physical processes we must assume, or demonstrate, that changes in *b*-value over time are meaningful. One potential problem is that if *b*-values are shown to change spatially, it may be difficult to determine whether they have also changed with time. The Augustine dataset presents us with a unique

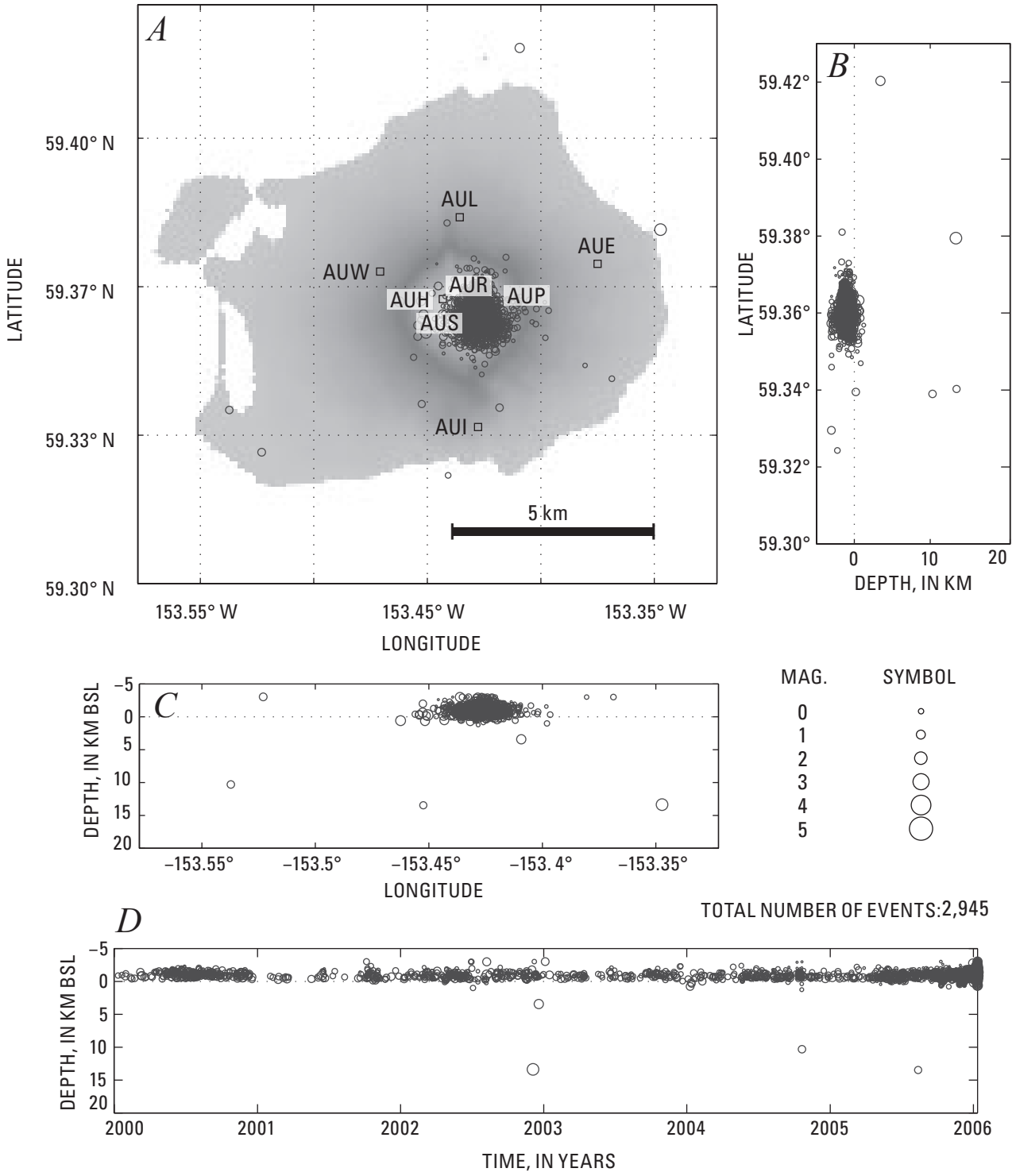

Figure 2. Summary plots of 2,945 earthquakes located by the Alaska Volcano Observatory near Augustine Volcano (shaded area is Augustine Island) from January 1, 2000, to January 11, 2006. Open circles show hypocenter locations. Hypocenters are scaled with magnitude (see scale). *A*, Earthquake epicenters in map view. *B* and *C*, north-south and east-west cross sections. *D*, Hypocenter focal depth plotted against time; a depth of 0 indicates sea level.

opportunity in this respect, because earthquakes located during the Augustine Volcano 2005–6 preeruptive swarm all occurred in a small seismic volume (fig. 2). The depth range for 95 percent of the earthquakes was confined to 0 to 2 km above sea level (asl), and depths appear to be constant over time. Despite the consistency, absolute depth control is poorly constrained and some earthquakes locate above the top of the volcano. In epicentral view the earthquakes span 1.5 km across the summit region. Some migration within this small volume is observed from late November 2005 to the onset of eruptive activity (DeShon and others, this volume; Power and Lalla, this volume). However, we believe that the seismic volume and the observed migration of events are small enough that we can consider the preeruptive swarm locations as essentially uniform in space.

The small seismic volume occupied by earthquakes at Augustine Volcano allows us to study the temporal evolution of *b*-values during the preeruptive earthquake swarm and compare our findings with information about temperature, pressure, and stress changes at Augustine. These other physical observations at the volcano will help to corroborate the temporal nature of observed *b*-value changes.

Methods

We first define a start date for the Augustine Volcano 2005–6 preeruptive earthquake swarm. Earthquake swarms are defined as increases in earthquake rates within a given volume over a relatively concentrated period of time without a single outstanding shock (Mogi, 1963). This is a rather loose definition and depends heavily on the opinions and perceptions of the reporter to define swarm durations. To lend a more quantitative element, we developed two algorithms, which used the daily number of located earthquakes to set a background rate and pick a swarm start date. We established the two algorithms to try to ensure that there was a real inflection or change at the selected point. Analysis of the years leading up to the 2005–6 activity was necessary to establish reliable background rates and give us a basis for determining change. A calendar year prior to the approximate onset of activity was used to establish background values used in each algorithm. Note that although only a single year is used to establish background rates in the algorithms, the earthquake rate at Augustine Volcano as seen in figures 1 and 2 appears to be relatively steady throughout the entire period from January 1, 2000, until the increase in activity in 2005. Late 2004 (October) is a possible exception to this statement; for details about this activity see Power and Lalla (this volume).

The first algorithm uses maximum daily event counts within a background period to establish a threshold for "increased activity." We call this method the largest-daily-count method (LDCM). In the case of Augustine all of these "counts" are located earthquakes, but the algorithm could potentially be used in places where earthquake locations are not possible. The second algorithm, the consecutive-days method (CDM), uses the low earthquake rate at Augustine Volcano to search for consecutive days with located earthquakes. Both the LDCM and CDM algorithms return a start date of April 30, 2005, for the beginning of the Augustine Volcano earthquake swarm. See appendix 1 for complete descriptions of the algorithms, flow chart diagrams, and additional details.

Using April 30, 2005, as the start date gives a total duration of 257 days for the preeruptive swarm. This long-building seismic swarm ultimately culminated in a very sharp increase in earthquake rate in the 13 hours directly preceding the eruption (Power and Lalla, this volume). For this paper we will term the 13-hour period of more energetic seismic activity on January 10–11, 2006, as the "short swarm" and refer to the swarm beginning April 30, 2005, as the "long swarm." This phenomenon of long and short swarms has been noted at many volcanoes (for both eruptive and non-eruptive swarm sequences), where either a long swarm, a short swarm, or both are present (Benoit and McNutt, 1996).

Calculations of *b*-value were carried out in ZMAP (Weimer, 2001). ZMAP is used to calculate a magnitude of completeness (M_c) for each *b*-value calculation, and only events above this threshold are used in the actual calculations (fig. 3). All *b*-values were determined using the maximum curvature method, which gives reasonable errors and is well suited for small earthquake catalogs and for temporal studies (Woessner and Wiemer, 2005). We also checked for station outages to ensure a uniform dataset. Although some station outages occur, we found no times when less than four seismometers were operating on Augustine Island. Four stations should generally be sufficient to determine consistent hypocenters and magnitudes (Lalla and Power, this volume).

To look for additional details, plots of *b*-value versus time were also generated using ZMAP (fig. 4). This calculation includes an automatic bootstrapping method to smooth the plot. A window size of 100 events with an overlap of 25 events was used to give the smallest time resolution possible. As with the standard *b*-value calculations, no cuts were made to the catalog, and the M_c was calculated for each time step.

Results

We found that the background (January 1, 2004–April 29, 2005) *b*-value was 1.51±0.1, the long swarm *b*-value was 1.26±0.04, and the short swarm *b*-value was 0.781±0.02 (fig. 3). A background calculation using all data between January 1, 2000, and April 29, 2005, yielded a *b*-value of 1.44±0.05, comparable to the background *b*-value which only uses data between January 1, 2004, and April 29, 2005. In addition to the low *b*-value for the short swarm, we also note the strange shape of its frequency-magnitude distribution curve (fig. 3*D*). The plot appears to have two separate slopes, a shallower slope for magnitudes up to 1.2 and a steeper slope for magnitudes greater than 1.2. The calculation of *b*-value with time shows an initial drop in *b*-value in mid-2004 and a dramatic

rise and fall in the *b*-value associated with the occurrence of the short swarm (fig.4).

To investigate the relationship between seismicity and deformation, we calculated the *b*-value for each of the three global positioning system (GPS) deformation stages as outlined by Cervelli and others (2006) (fig. 5). For stage 1 (constant slow inflation from June 1, 2005, to November 17, 2005) a *b*-value of 1.31±0.06 was calculated. The calculation for stage 2 (increased inflation possibly due to dike intrusion, from November 17, 2005 to December 10, 2005) yielded a *b*-value of 1.85±0.1. Finally, stage 3 (constant from December 10, 2005 to January 11, 2006) gave a *b*-value of 1.18±0.05. Data from the short swarm on January 10–11, 2006, was left out of this *b*-value calculation for stage 3 because of the odd frequency-magnitude distribution (fig. 3D).

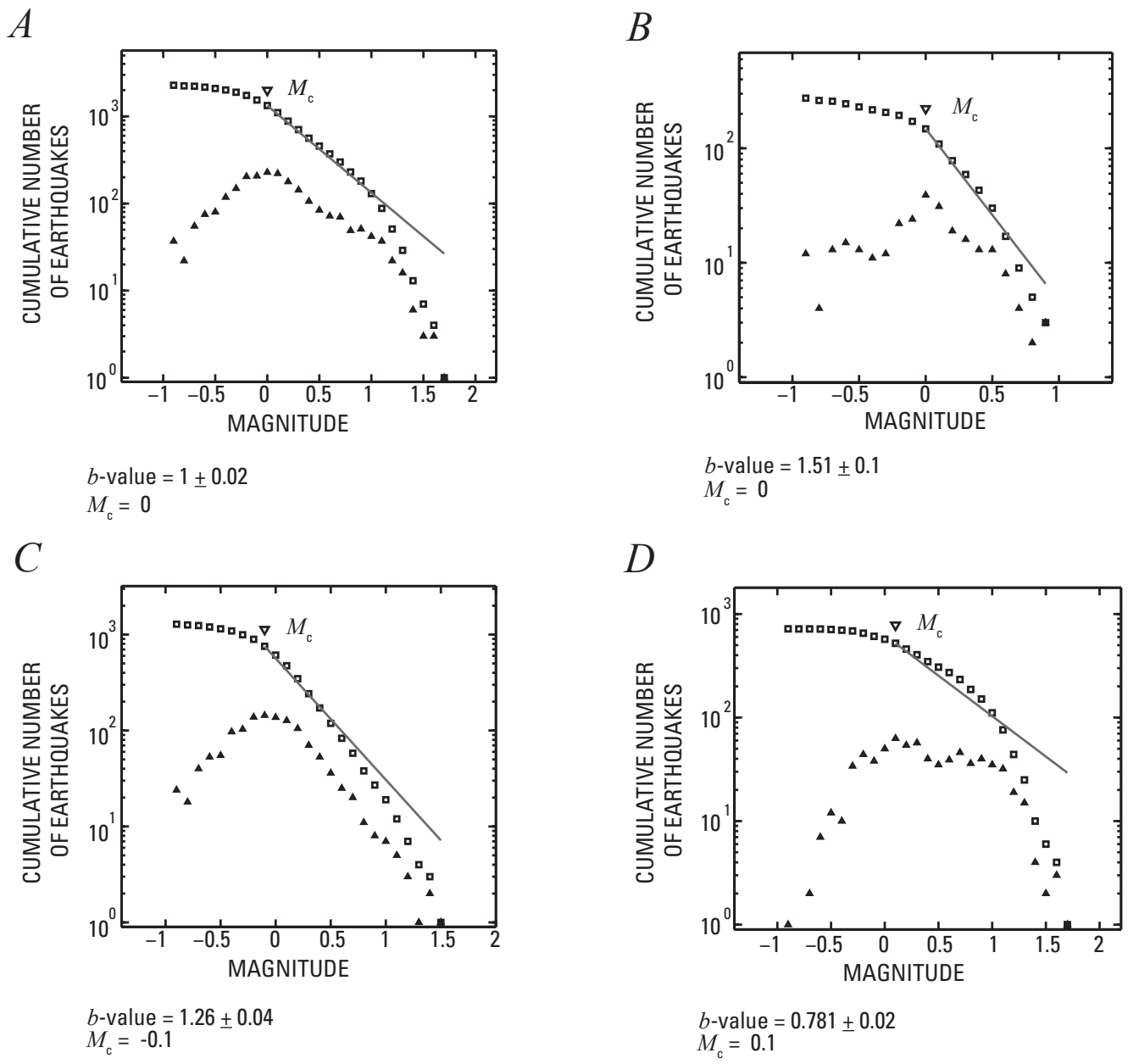

Figure 3. Cumulative frequency plots of Augustine earthquakes from January 1, 2000 to the initial eruption on January 11, 2006 with derived *b*-values. Triangles and squares show the number of earthquakes at each magnitude and the cumulative number of earthquakes, respectively. The magnitude of completeness (M_c) is shown by an inverted triangle; errors in *b*-value calculations reflect the 95-percent confidence interval of the maximum likelihood solution. *A*, The entire AVO earthquake catalog (January 1, 2000 to January 11, 2006). *B*, The background (January 1, 2000 to April 29, 2005). *C*, The long swarm (April 30, 2005 to January 10, 2006). *D*, The short swarm (13 hours prior to the initial eruption on January 11, 2006).

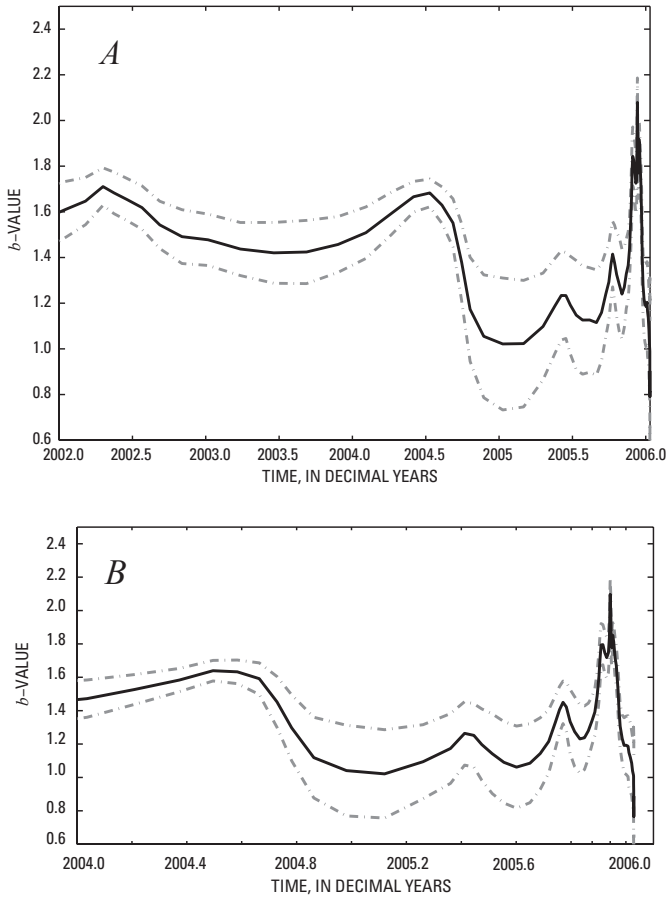

Figure 4. Plots of *b*-value with time for Augustine earthquakes. *A*, For time interval 2002–6. The calculation uses a moving window of 100 earthquakes with an overlap of 25 events. The solid line is the calculated *b*-value, and the dashed lines indicate the 95-percent confidence interval of the maximum likelihood solution. *B*, Data for 2004–6 expanded for more detail.

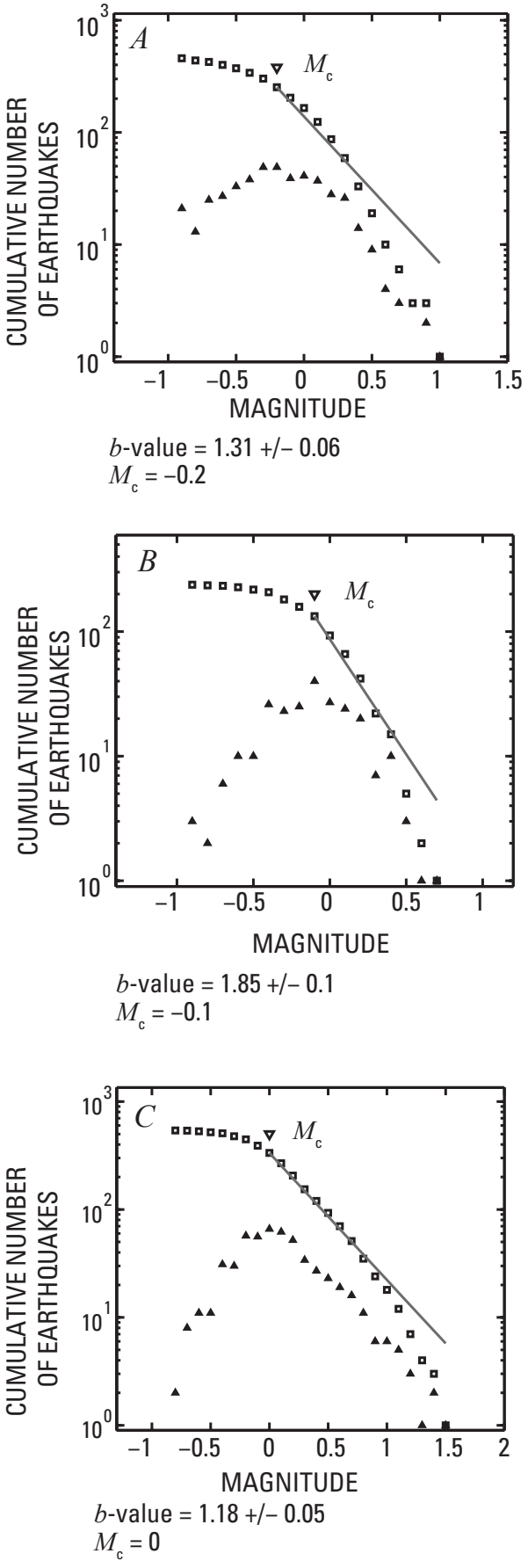

Figure 5. Results of *b*-value calculations for each precursory deformation stage outlined by Cervelli and others (2006). M_c is magnitude of completeness, and errors in *b*-value calculations reflect the 95-percent confidence interval of the maximum likelihood solution. *A*, Stage 1 (constant slow inflation from June 1, 2005, to November 17, 2005) *B*, Stage 2 (increased inflation possibly due to dike intrusion from November 17, 2005, to December 10, 2005) *C*, Stage 3 (continually increasing inflation from December 10, 2005, to January 11, 2006).

Discussion

Several physical processes could be associated with each part of an earthquake swarm. We expected to see an increase in stress in the surrounding region caused by pressurization of a deeper magma chamber during the long (building) swarm. This would lead to an overall decrease in the *b*-value. It was also expected that this would be followed by an increase in pore pressure and thermal gradient as the magma moved closer to the surface shortly before the eruption. These final changes would accompany the short swarm and cause an increase in the *b*-value above previous levels. These concepts are illustrated schematically in figure 6. Our results given earlier differ from this conceptual model. Neither the long swarm nor the short swarm shows an overall increase in *b*-value and it is the short swarm that has the lowest *b*-value of all the three periods. We will now examine these differences between our model and results by looking at the long and short swarms separately and then discussing our overall conclusions.

Long Swarm

We see in the plot of *b*-value versus time (fig. 4) that there is an initial drop in *b*-value in late 2004, but it precedes the actual seismic-swarm onset (April 30, 2005). A decrease in the *b*-value prior to the long swarm may explain why the long swarm does not have a *b*-value lower than the background period in the standard calculations. We will look to corroborate the timing of the *b*-value drop through correlation with other physical observations made at Augustine.

The *b*-values associated with the three precursory deformation stages help to identify some physical processes at work during the long swarm. The second stage of activity, from November 17, 2005, to December 10, 2005, has a higher *b*-value than the other two stages. Higher *b*-values are often associated with high thermal gradients and increases in pore pressure (Warren and Latham, 1970; Wyss 1973). At Augustine, the higher *b*-value could be explained as a result of pressurization that was caused by the inferred dike emplacement (Cervelli and others, 2006; Cervelli and others, this volume). An increase in pore pressure is likely to have occurred preceding the 75-km-long steam plume seen on December 12, 2005, in 250-m MODIS data (Bailey and others, this volume). The increase in *b*-value is also seen in figure 7, which shows the three deformation stages superimposed onto the plot of *b*-value with time. While the general trends in the *b*-value seem to correlate well, figure 7 also illustrates that they do not correlate exactly with the deformation changes, and there are additional changes in *b*-value that are not accompanied by any apparent changes in deformation.

Another physical observation at Augustine was an increase in temperature, at seismic station AUS (see fig. 2 for seismic-station locations). The hut at seismic station AUS contained a thermistor (LM335A thermocouple paired with a 3.3-kohm 5-percent resistor, manufactured by National Semiconductor) in the McVCO (a microcontroller-based frequency generator that replaces the voltage controlled oscillator (VCO) used in the analog telemetry of seismic data), which is used to test station health. The McVCO was located on a battery rack inside the AUS seismic hut, approximately 1.4 m off the ground. The LM335A works over a temperature range of –40 to 100°C and is accurate within 1°C. Temperature information from the thermistor was received with the calibration pulse, every 12 hours from late October 2000 through the eruption on January 11, 2006. No changes were made in the processing of this data from October 2000 through January 2006 when the AUS hut was destroyed (G. Tytgat, oral commun., 2006). Regional air temperature data from Homer, Iliamna, and Seldovia, courtesy of the Alaska Climate Data Center, and data from a National Oceanic and Atmospheric Administration (NOAA) weather station on Augustine Island

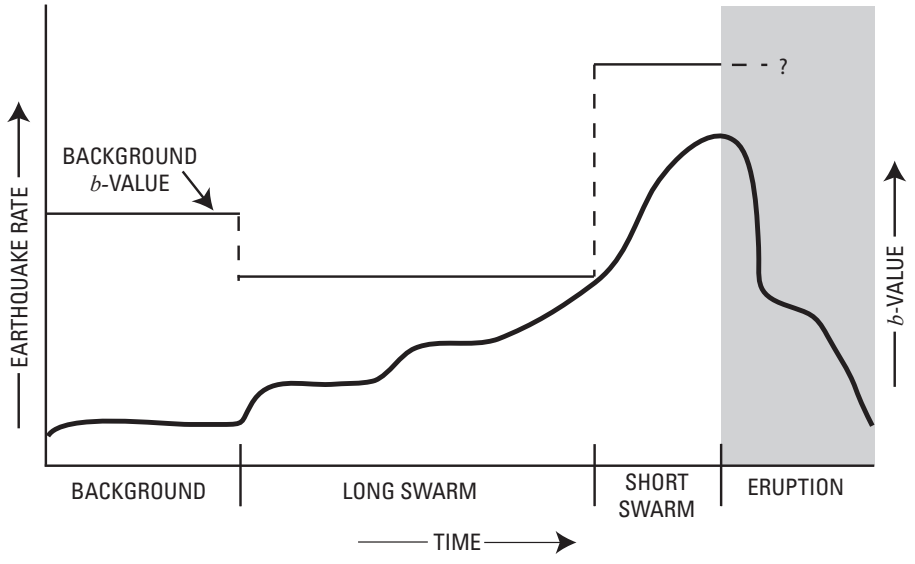

Figure 6. Schematic diagram illustrating how we expected the *b*-value to change over the course of the precursory earthquake swarm at Augustine Volcano. Curved line indicates the observed earthquake rate, and the straight horizontal lines indicate relative *b*-value changes expected for each part of the swarm activity.

were also processed for comparison with the recorded AUS temperatures.

The weather stations at Homer, Iliamna, Seldovia, and the Augustine NOAA station all gave temperatures that agreed with one another and varied systematically with the season. However, the changes seen at the AUS seismic hut differed from the others and are likely volcanic in origin. In figure 8 daily maximum temperatures from the three regional stations and the NOAA weather station on Augustine Island are plotted and overlain with weekly temperature averages from the AUS hut. Where data were unreported for a period, the average of the existing data within the 7-day period is shown instead. Periods where no data were reported are plotted as a zero value for both the regional stations and the AUS site. The long outage in AUS data in 2002 is a period when no data were received. Data were transmitted during the outage in 2004, but the temperature sensor did not report temperatures. These times do not correspond to the catalog-reported station outages (Dixon and others, 2008) and are more likely to be related to weather interference with the signal or a problem with the temperature sensor itself. Table 1 shows monthly average temperatures from January 2002 through January 2006. The monthly average shows a marked increase beginning in January 2005. A smaller increase of approximately 5°C is also seen in November and December 2004. This can also be seen in figure 9, where monthly averages of AUS hut temperatures from January 2002 through January 2006 are overlaid on the plot of *b*-values. Again, the monthly average shows a marked increase beginning in January 2005, and a smaller increase of approximately 5°C is also seen in November and December 2004.

Table 1. Monthly averaged temperatures at seismic station AUS on Augustine Volcano from January 2002 through January 2006.

[The value for January 2006 is only an average through January 11. All other values span the entire month. An asterisk indicates insufficient data to calculate the monthly average.]

	Average Temperature (°C)				
Month	**2002**	**2003**	**2004**	**2005**	**2006**
January	6.18	5.72	2.57	29.90	45.28
February	6.95	7.22	6.96	30.74	
March	5.74	2.83	1.55	35.75	
April	6.74	6.75	7.19	34.34	
May	4.31	8.82	11.00	28.35	
June	4.25	7.83	11.31	33.45	
July	*	13.51	15.04	39.03	
August	*	13.07	19.47	39.09	
September	6.96	8.78	12.09	33.39	
October	4.55	4.74	*	30.33	
November	5.28	3.87	13.70	24.26	
December	6.00	3.74	10.79	44.31	

An ASTER (advanced spaceborne thermal emission and reflection radiometer) image acquired on December 20, 2005, and the first FLIR (forward looking infrared radiometer) mission during the Augustine unrest on December 22, 2005, both revealed areas of warm, bare rock and active fumaroles. The FLIR observations recorded bare rock temperatures of 10°C and fumarole temperatures as high as 210°C (Wessels and others, this volume). These observations confirm that summit temperatures were

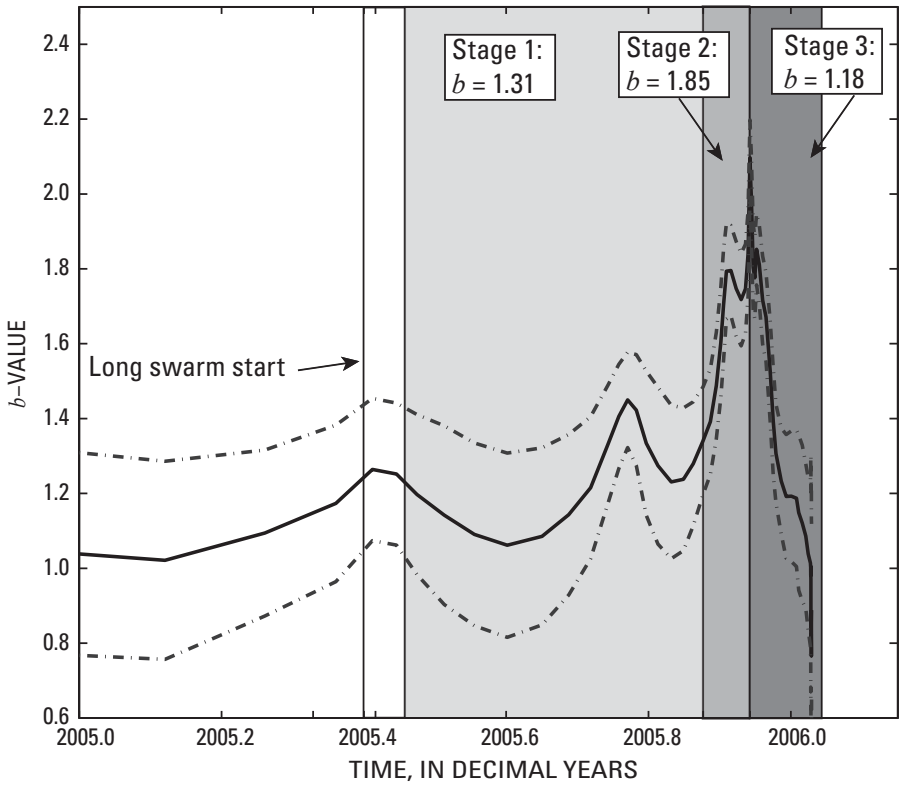

Figure 7. Plot of calculated *b*-value with respect to time for 2005–6, overlaid with shaded boxes indicating the periods of the long swarm and each of the three precursory deformation stages outlined in Cervelli and others (2006). The solid line is the calculated *b*-value, and the dashed lines indicate the 95-percent confidence interval of the maximum likelihood solution.

already elevated by late December. The AUS temperatures reported for those days were 44.6°C and 46.3°C, respectively. The consistency of data processing and a visit to the summit in December 2005 also provide evidence that this was a real thermal change (G. Tytgat and E. Clark, oral commun., 2006). The temperature change coincides with the initial *b*-value change in late 2004, which we see in our *b*-versus-time calculations. This change in *b*-value is possible evidence for a change in heat or fluid movement at depth at Augustine Volcano prior to the beginning of the seismic swarm.

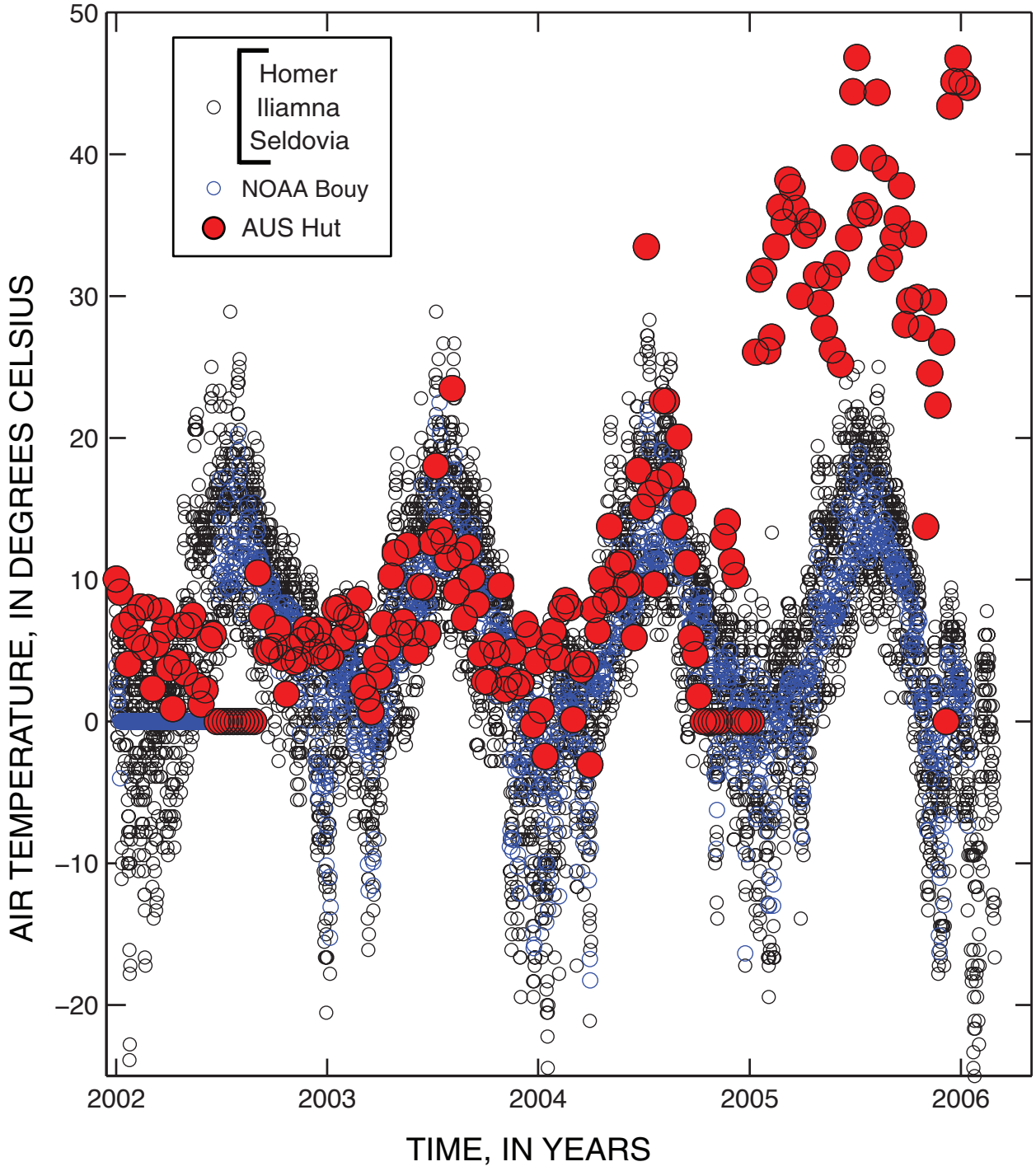

Figure 8. Plot of daily maximum air temperatures recorded in nearby communities (Homer, Iliamna, and Seldovia), at the Augustine Island NOAA weather station, and 7-day average temperatures from the seismic station AUS near the summit of Augustine Volcano. Tick marks on the horizontal axis mark the beginning of each year.

Given that the initial *b*-value decrease and temperature increase appear to be linked, we face the question, why does the *b*-value decrease? For *b*-value changes associated strictly with an increasing thermal gradient, the value of *b* should increase (Warren and Latham, 1970), the opposite of what we observe. We interpret this downward *b*-value trend to reflect an increase in stress throughout the seismic volume caused by the same physical process that is changing the thermal gradient. This suggests a possible influx of magma at depth or some other process that increases both thermal gradient and stress. Further support for a stress-induced *b*-value change is found in the slight time difference between the initial *b*-value change and the onset of the temperature increase seen in figure 9. A stress change would likely propagate instantaneously throughout the affected volume, whereas thermal (and pore pressure) effects take time to propagate through a volume of rock. Observing a stress change in *b*-values while we have evidence of thermal changes implies that stress effects dominate *b*-value observations when both parameters are changing simultaneously.

Because of the apparent importance of stress in overall *b*-value observations and past studies by Roman and others (2004), which suggest changes in stress tensors during periods of unrest and eruption, we undertook a study of focal mechanisms at Augustine. Determination of correct polarization of stations, normal or reversed, was made by looking at 37 large teleseisms from 2002 to 2006. *P*-wave polarities were then repicked for all located earthquakes for which at least six clear *P*-wave first motions were possible. Once the *P*-wave motions were repicked, the events were relocated using the same velocity model and processing steps as for the initial catalog locations (Dixon and others, 2008).

Focal mechanisms were computed for all earthquakes using FPFIT (Reasenberg and Oppenheimer, 1985). Solutions were judged acceptable if they had: a misfit of less than 0.15 (less than 15 percent of stations inconsistent with the preferred solutions); STDR (distribution around the hypocenter) ≥ 0.40; and an average uncertainty in strike, dip, and rake of $\leq 25°$.

After applying this criteria, 79 out of 201 earthquakes returned acceptable focal-mechanism solutions. There were 19 events (out of 61 picked) with acceptable solutions from 2002 through 2004 and 60 events (out of 140 picked) from the long swarm (all events with acceptable solutions in 2005 occurred during the long swarm). Appendix 2 shows all 79 acceptable

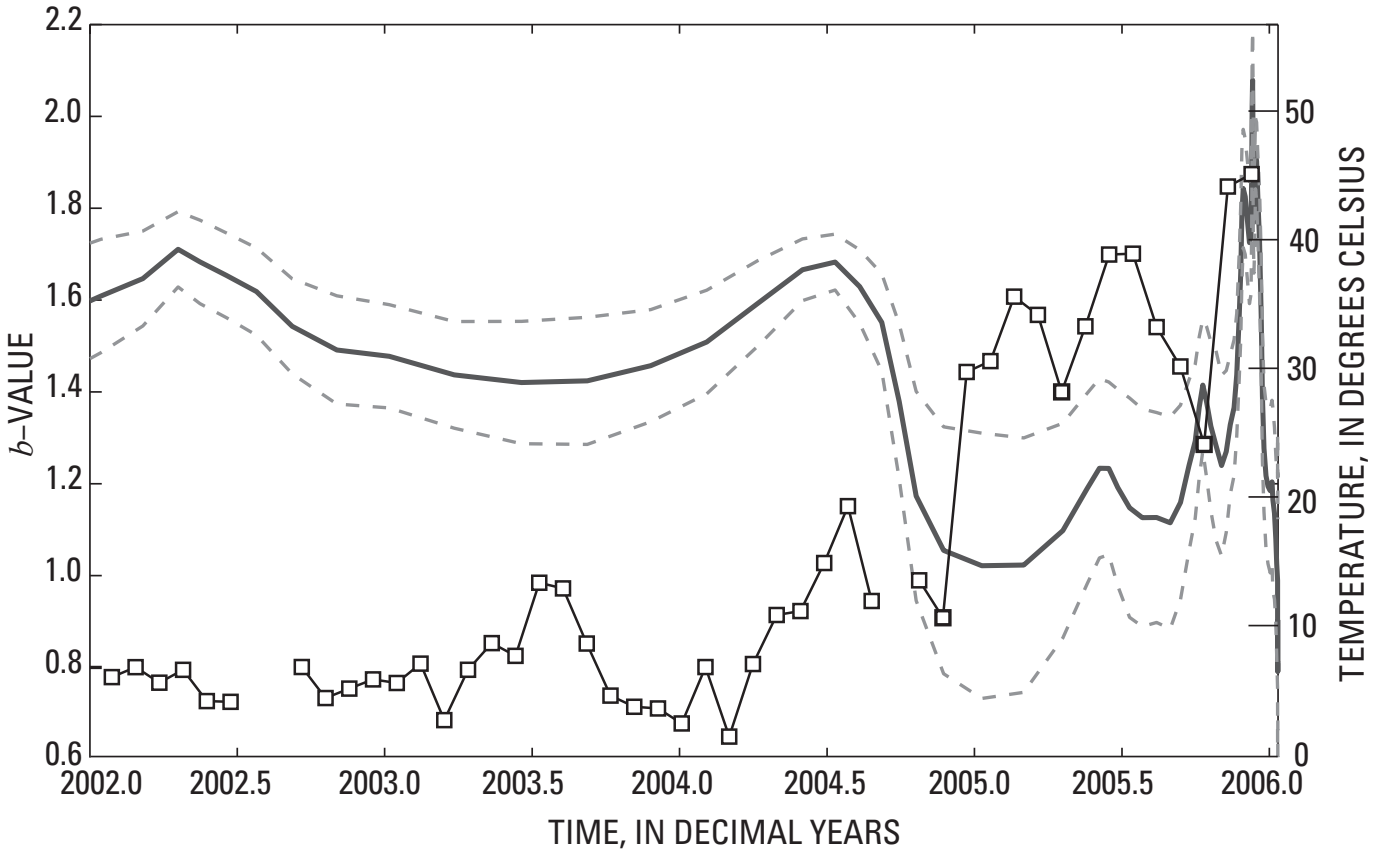

Figure 9. Plot of *b*-value with time from figure 4 (shown in boldline), overlaid with monthly average temperatures (as squares) from a thermistor at seismic station AUS. The *b*-value calculation uses a moving window of 100 earthquakes with an overlap of 25 events, and the dotted lines represent the 95-percent confidence interval of the maximum likelihood solution.

focal mechanisms. Stress tensor inversions were attempted in ZMAP for both the background data (2002 to 2004) and the long swarm (2005 through January 10, 2006) using the method of Michael (1987). The inversions had very high errors and do not display a dominant faulting style. The lack of any pattern or observable change in the focal mechanisms with time and the highly variable stress tensors agree with work by DeShon and others (this volume), which suggests no dominant faulting style or area within the Augustine Volcano seismic volume.

Short Swarm

In our conceptual model we expected the *b*-value of the short swarm to be the highest of all the time periods (fig. 6), and yet our results show that it is the lowest (fig. 3). We also see this low value in the calculation of *b*-value versus time, where there is a dramatic drop in *b*-value just before the eruption (fig. 4). We also note, however, that there is a strange bend or knee in the *b*-value curve (fig. 3*D*). This led us to question whether the low value was real and whether there was an "excess" of larger events occurring, or if this lower value was an artifact of a poor fit to a single distribution. Upon examining magnitudes with time, we find that the decrease in *b*-value leading into the eruption is real and appears to be caused by an increase in the number of $M_L \geq 1$ events (large earthquakes for Augustine) that occur in that time frame.

Having convinced ourselves that the observed low *b*-value for the short swarm is real, we look for ways to explain the observed knee in the frequency-magnitude distribution. Bends or knees like this one (fig. 3*D*) have been observed at other volcanoes, including Mount St. Helens (Qamar and others, 1983), Fernandina (Filson and others, 1973), and Usu (Okada and others, 1981; Okada 1983). At Fernandina the data are directly related to caldera collapse (Filson and others, 1973), so we will not seek comparisons with their conclusions. Okada and others (1981) outlined the appearance of odd frequency-magnitude plots at Usu and found that there were distinct earthquake families occurring in time. These earthquake families accounted for an unusually high number of earthquakes with similar magnitudes. Work by Buurman and West (this volume) and DeShon and others (this volume) indicates that earthquake families were occurring at Augustine from 1993 through 2006. Buurman and West (this volume) identified seven families on January 10–11, 2006, before the first eruption. Because only 41 out of 722 located earthquakes appear in the families on January 10–11, 2006, we conclude that earthquake families alone cannot explain the unusual shape of the frequency-magnitude plot.

The knee in the Mount St. Helens data corresponds to a group of earthquakes with magnitudes 4.5 and greater (Qamar and others, 1983). Low-frequency energy also accompanies many of the located earthquakes, and an increase in the low-to high-frequency amplitude ratio is observed leading up to the eruption. This has been interpreted as either the source of earthquakes becoming shallower or evidence of the magma chamber expanding (Qamar and others, 1983; Main, 1987).

A magnitude histogram for the short swarm is shown in figure 10. Most complete earthquake catalogs have a single normal-shaped distribution. The bell-shaped curve results from the lack of complete detection for magnitudes below the M_c and a similar reflected exponential decay of higher magnitudes resulting from decreasing frequency of occurrence. The histogram of the January 10–11, 2006, earthquakes is clearly not a single peaked bell-shaped curve and appears to be bimodal.

A separate study of very long period (VLP) energy was performed to investigate possible VLP energy associated with some of the high-frequency earthquakes during the short swarm, first observed by S. DeAngelis and J. Power (oral. commun., 2007). We looked for VLP signals during the short swarm (January 10–11, 2006) using data from temporary broadband stations AU11, AU12, AU13, AU14, and AU15 (for locations of these stations, see Power and Lalla, this volume). These seismometers were installed on Augustine Island in response to the increasing earthquake activity in December of 2005 and were not telemetered (Power and others, 2006). Initially we chose two different filters, a band pass filter from 0.01 to 0.2 Hz, and a second separate low pass filter of 0.05 Hz. The low pass filter

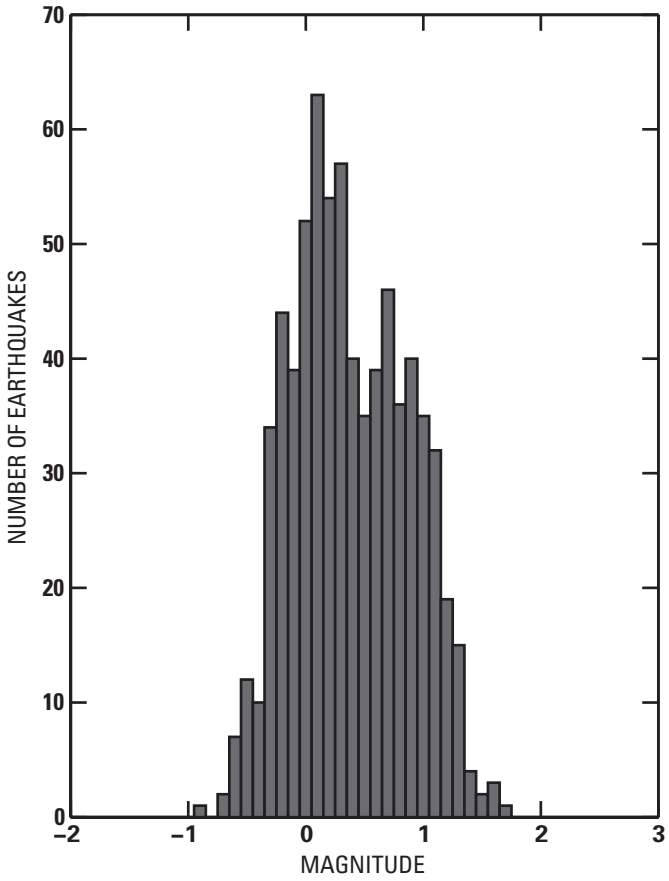

Figure 10. Histogram of magnitudes for located earthquakes at Augustine Volcano from the 13-hour short swarm on January 10–11, 2006.

of 0.05 Hz, corresponding to periods of 20 seconds and greater, showed the most consistent and largest amount of energy, and we chose that filter to examine all of the data.

To establish whether or not VLP energy was accompanying the high-frequency located earthquakes during the short swarm, we looked through continuous data at the time of each located earthquake, applied a 0.05 Hz low pass filter, and visually determined whether or not there was a pulse of VLP energy. No quantitative criteria were assigned for either amplitude or wavelength. Short-period stations AUP and AUW were used to verify the position of located earthquakes because the temporary broadband stations were not used for the location of earthquakes in the catalog. There were other long-period and VLP signals seen during this time frame, but no events without accompanying located high-frequency earthquakes were considered in this study. Figure 11 shows raw and filtered waveforms for several earthquakes at Augustine Volcano.

Using this method we found that 221 out of 722 located earthquakes during the short swarm had accompanying VLP energy. The events were separated according to this classification, and the individual properties of each group were examined. A magnitude histogram was created for each set of events, and these are plotted in figure 12. Both sets of events gave approximately normal distributions, indicating that they are complete populations of events. Furthermore, the two sets of events have notably different mean magnitudes. The smallest event without accompanying VLP energy is M_L 0.1, while the smallest event observed with VLP energy is M_L 0.9.

To test the significance of this apparent difference in mean magnitude, a Student t-test was run (Davis, 2002). This test examines the likelihood that two populations have come from a single parent population. The mean magnitude of the events with VLP energy was 0.91, and the mean magnitude of events without observed VLP energy was 0.16 (negative magnitudes

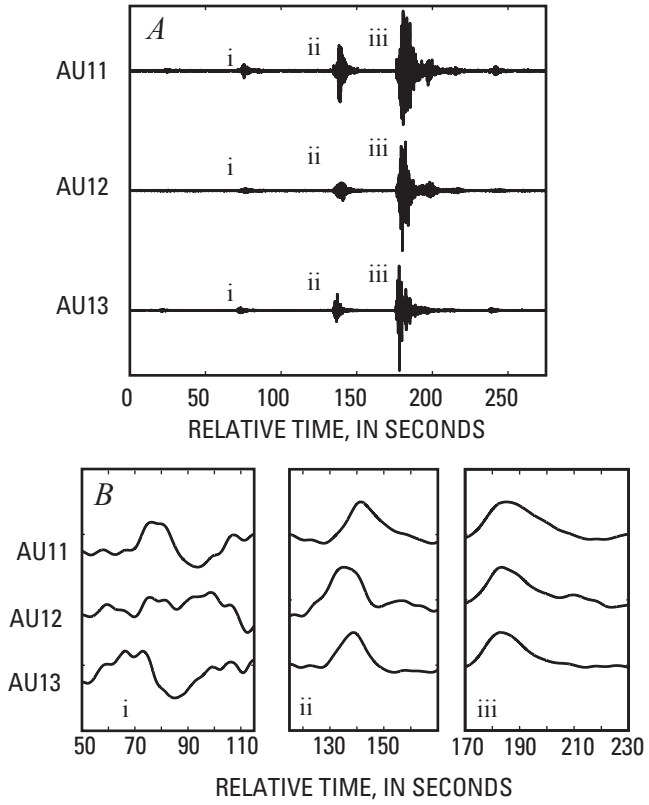

Figure 11. Waveforms for three located earthquakes at Augustine Volcano on January 10, 2006, as recorded on stations AU11, AU12, and AU13. The calculated origin time, depth, and magnitude are 19:48:58, 19:50:02, and 19:50:43 AKST; –0.57, –0.84, and –0.57 km below sea level; and 0.6, 0.6, and 1.4, respectively for the three earthquakes. *A,* Unfiltered waveforms at each station. *B,* Filtered waveforms around each earthquake that have been normalized to the maximum amplitude within the sample and low–pass filtered at 0.05 s for each station. Note that the first event shows no coherent VLP energy while the second and third events have significant VLP energy.

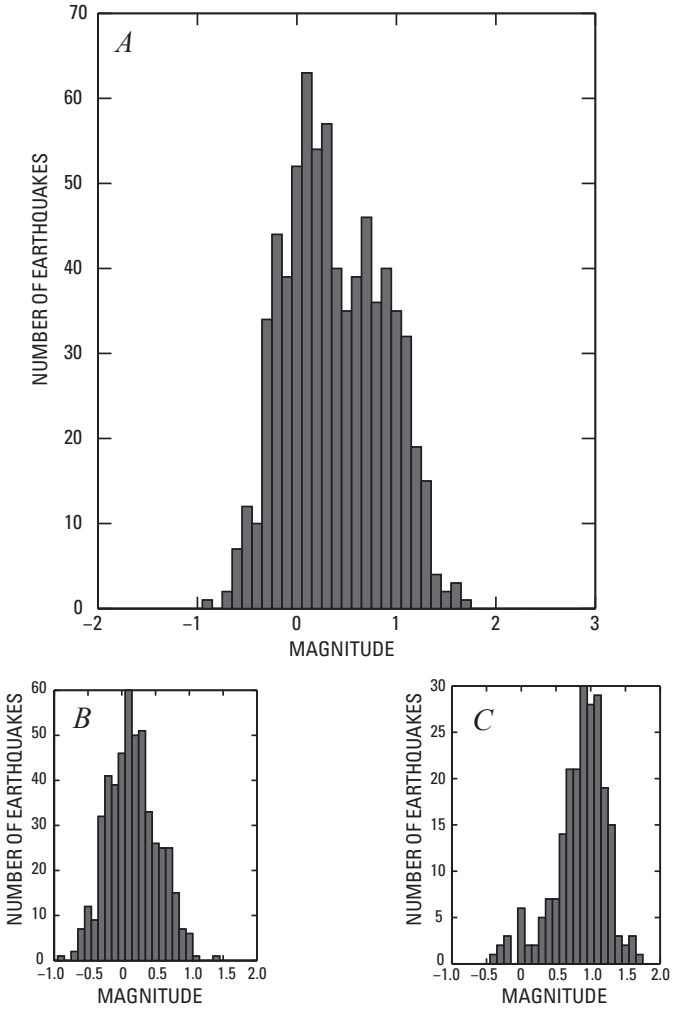

Figure 12. Magnitude histograms for (*A*) All events at Augustine Volcano during the short swarm (January 10–11, 2006), (*B*) Events with associated very long period energy, and (*C*) events without any associated very long period energy.

reduce the overall mean). The Student t-test produced a value of 26.3, well above the limit of 3.09 for a statistically significant difference between the means. Thus the two sets of earthquakes represent different parent populations.

To quantify the differences in energy implied by the differences in mean magnitude, we used ZMAP to calculate the cumulative moment for each earthquake population (fig. 13). The population with VLP energy has a moment of 1.01×10^{14} Nm, a factor of four larger than the cumulative seismic moment for the events without VLP energy (2.46×10^{13} Nm). The VLP events are also found to have more than half of the total moment for the entire seismic swarm and slightly more energy than all other earthquakes from January 1, 2000, through the January 11, 2006, eruption (9.49×10^{13} Nm).

Having observed that both events with and without VLP energy appear to have bell-shaped distributions (fig. 12), we note that the population without VLP energy represents earthquake activity on January 10–11, 2006, without the excess higher magnitude events that earlier made the observed magnitude histogram appear bimodal. The population with VLP energy, that has significantly higher magnitudes, corresponds to the $M \geq 1.0$ events that are seen to drive down the *b*-value for the short swarm. Essentially the population of VLP events is the "cause" of the bimodal magnitude histogram and of the associated low *b*-value for the short swarm.

The occurrence of VLP energy accompanying earthquakes and a bimodal *b*-value are in good agreement with the findings at Mount St. Helens (Qamar and others, 1983; Main, 1987), where both a bimodal frequency-magnitude distribution and the occurrence of lower frequency energy accompanying some of the recorded earthquakes were observed. Further comparison between these findings is ongoing.

The fact that the population of events without VLP energy has a similar M_c as the events in the long swarm suggests that the underlying process driving the long swarm continued during the short swarm and an additional population of earthquakes (those with VLP energy) was superimposed onto the existing seismicity trend. We believe that this is evidence of independent concurrent seismogenic processes at Augustine preceding the eruption. The fact that both sets of events appear to be happening in the same volume indicates that there is probably a difference in their mechanisms. Following Scholz (1968), we interpret the low *b*-values and larger event sizes of the VLP population to represent the formation of new fractures. The larger event size is required to accompany the low *b*-value because breaking rock, as opposed to failure along pre-existing fractures, requires much more energy.

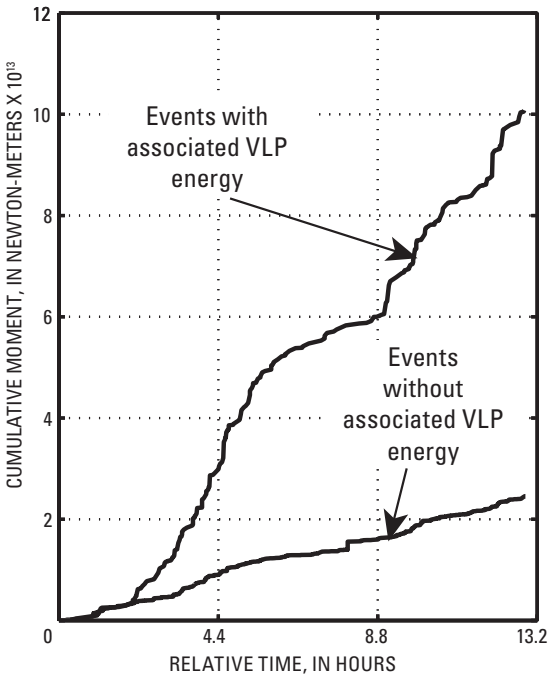

Figure 13. Cumulative seismic moment for earthquakes with and without associated very long period energy during the 13-hour short swarm on January 10–11, 2006. Time is shown in hours relative to the beginning of the short swarm at 1535 AKST on January 10.

A lull in earthquake rate is noted about 8 hours into the short swarm, and it appears in both populations of events (fig. 14). No major changes in depth or magnitude are seen in either population before or after the lull. Figure 15 shows several plots comparing the rate at which the two populations of events were occurring with time. We infer from the lack of change in either population that the individual processes causing each population of events did not change either. This indicates that the lull was not caused by a change in process and was probably the result of a mechanical, material, or thermal barrier present at Augustine Volcano.

Focal mechanisms were not attempted for the earthquakes during the short swarm. No clear stress tensor was produced from analysis of the background or long swarm, and so even if a stress tensor was produced from the short swarm, there would be no way to compare it to the preceding time periods.

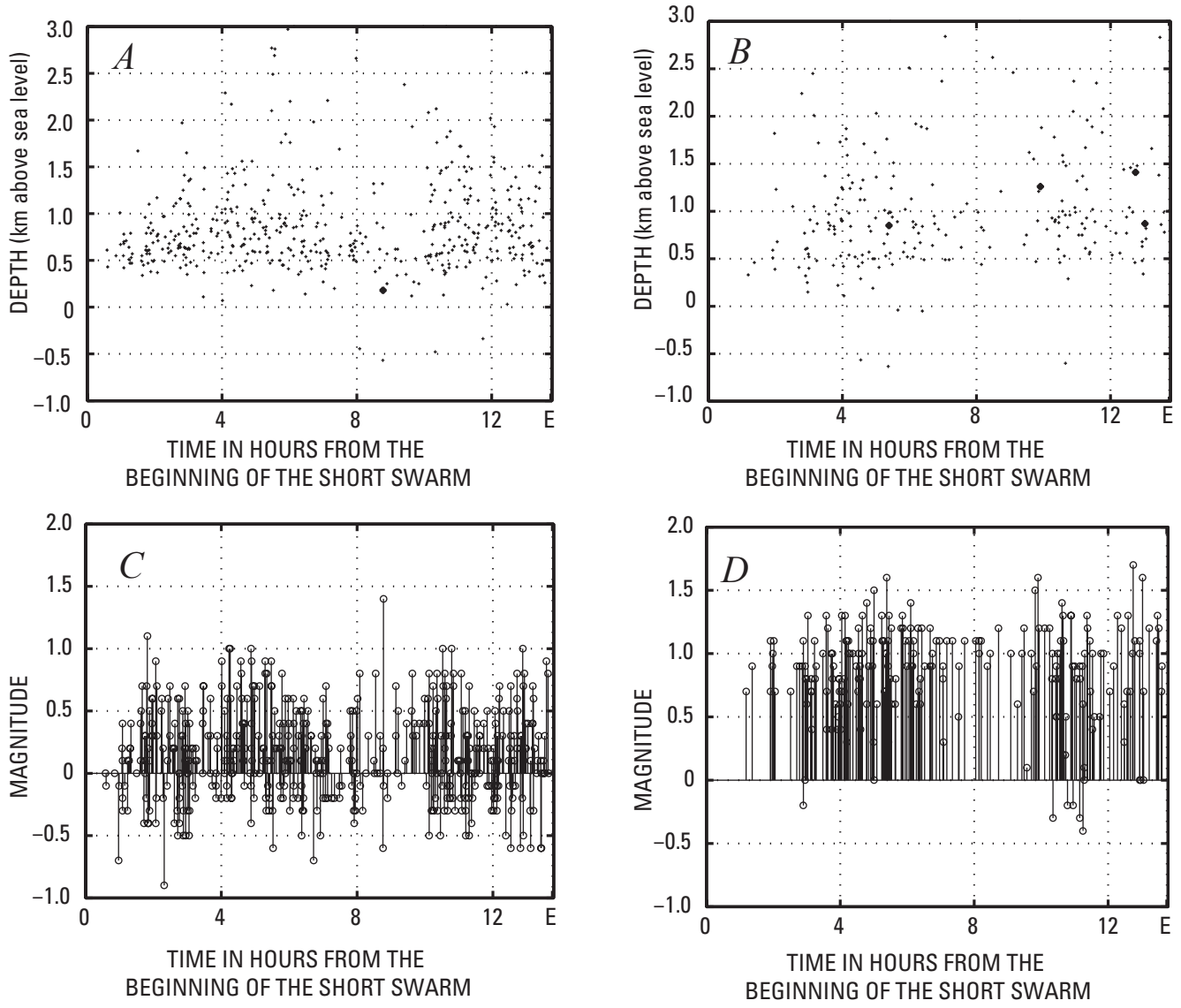

Figure 14. Plots of earthquake focal depth with time and of magnitude with time plots for events with very long period (VLP) energy (*A* and *C)* and without VLP energy (*B* and *D)*. The time axis reflects the time since the onset of the short swarm, taken to be at 1535 AKST on January 10, 2006. "E" marks the initiation of explosive activity.

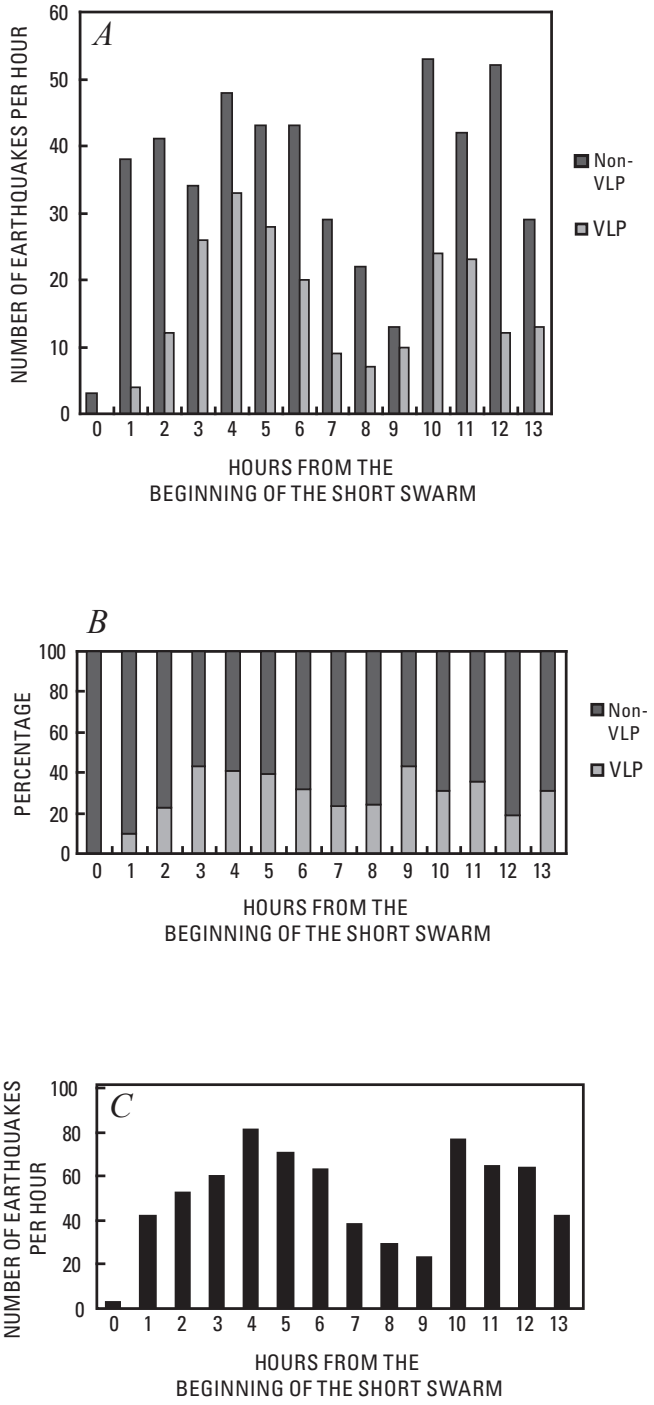

Figure 15. Summary plots the occurrence of earthquakes with very long period (VLP) and non-VLP energy during the 13-hour-long short swarm on January 10-11, 2006. *A*, histogram showing the number of earthquakes per hour with and without very-long-period energy. *B*, Percentage per hour of the two populations of earthquakes. *C*, Histogram showing the total number of earthquakes recorded per hour. Note that the total number of earthquakes in *C* tends to mirror the percentage of VLP events in *B* with a slight time delay.

Conclusions

We have been able to identify changes in *b*-value during the Augustine preeruptive earthquake swarm that we believe were caused by changes in thermal gradient, pore pressure, and stress. These changes have been substantiated through comparison with other physical observations at Augustine Volcano. Our observations in conjunction with temperatures recorded on Augustine Island suggest that when thermal-gradient and stress changes occur simultaneously, stress dominates the overall *b*-value observations. We have also been able to identify a unique set of high-frequency earthquakes that have associated VLP energy. These events are a complete and separate population from other high-frequency earthquakes occurring during the short swarm. The VLP events have significantly higher energy release than other earthquakes, and we believe that they may be the primary expression of magma moving towards the surface. We see preliminary evidence to suggest that *b*-value changes can precede other more obvious punctuations in activity, such as the onset of the seismic swarm. Changes in *b*-values can be used to corroborate other physical observations, such as the *b*-value changes that accompanied temperature changes or increased steaming before the large steam plume on December 12, 2005. These *b*-value changes may indicate that larger or deeper processes are occurring than can otherwise be observed. In this way *b*-value calculations can give us more information about the causes and physical process at work during earthquake swarms. Given these findings we suggest that systematic evaluation of *b*-values become a more regular part of monitoring efforts.

Acknowledgments

Thank you to Matt Haney, Seth Moran, and John Power for their reviews, which helped to shape this paper. We acknowledge the AVO staff, especially Scott Stihler, Guy Tytgat, Ed Clark, and Jim Dixon. During the course of this work we also had discussions with Mike West, Doug Christensen, Stephanie Prejean, Helena Buurman, Lea Burris, Celso Reyes, Matt Gardine, Nicole DeRoin, Tanja Peteresen, Silvio DeAngelis, and others.

References Cited

Bailey, J.E., Dean, K.G., Dehn, J., and Webely, P.W., 2010, Integrated satellite observations of the 2006 eruption of Augustine Volcano, *in* Power, J.A., Coombs, M.L., and Freymueller, J.T., eds., The 2006 eruption of Augustine Volcano, Alaska: U.S. Geological Survey Professional Paper 1769 (this volume).

Bath. M., 1981, Earthquake magnitude—recent research and current trends: Earth Science Review, v. 17, p. 315–98.

Benoit, J.P., and McNutt, S.R., 1996, Global volcanic earthquake swarm database, 1979–1989: U.S. Geological Survey Open-File Report 96-0069, 333 p.

Buurman, H., and West, M.E., 2010 Seismic precursors to volcanic explosions during the 2006 eruption of Augustine Volcano, *in* Power, J.A., Coombs, M.L., and Freymueller, J.T., eds., The 2006 eruption of Augustine Volcano, Alaska: U.S. Geological Survey Professional Paper 1769 (this volume).

Cervelli, P.F., Fournier, T.J., Freymueller, J.T., and Power, J.A., 2006, Ground deformation associated with the precursory unrest and early phases of the January 2006 eruption of Augustine Volcano, Alaska: Geophysical Research Letters, v. 33, doi: 10.1029/2006GL027219.

Cervelli, P.F., Fournier, T.J., Freymueller, J.T., Power, J.A., Lisowski, M., and Pauk, B.A., 2010, Geodetic constraints on magma movement and withdrawal during the 2006 eruption of Augustine Volcano, *in* Power, J.A., Coombs, M.L., and Freymueller, J.T., eds., The 2006 eruption of Augustine Volcano, Alaska: U.S. Geological Survey Professional Paper 1769 (this volume).

Davis, J.C., 2002, Statistics and data analysis in geology: New York, J. Wiley, p. 68–74.

DeShon, H.R., Thurber, C.H., and Power, J.A., 2010, Earthquake waveform similarity and evolution at Augustine Volcano from 1993 to 2006, *in* Power, J.A., Coombs, M.L., and Freymueller, J.T., eds., The 2006 eruption of Augustine Volcano, Alaska: U.S. Geological Survey Professional Paper 1769 (this volume).

Dixon, J.P., Stihler, S.D., Power, J.A., and Searcy, C., 2008, Catalog of earthquake hypocenters at Alaskan Volcanoes; January 1 through December 31, 2006: U.S. Geological Survey Data Series 326, 78 p.

Filson, J., Simkin, T., and Leu, L.-K., 1973, Seismicity of a caldera collapse—Galapagos Islands 1968: Journal of Geophysical Research, v. 34, p. 8591–8622.

Gutenberg, R., and Richter, C.F., 1944, Frequency of earthquakes in California: Bulletin of the Seismological Society of America, v. 34, p. 185–188.

Ishimoto, M., and Ida, K., 1939, Observations of earthquakes registered with the microseismograph constructed recently: Bulletin of the Earthquake Research Institute, University of Tokyo, v. 17, p. 443–478.

Jolly, A.D., and McNutt, S.R., 1999, Seismicity at the volcanoes of Katmai National Park, Alaska; July 1995–December 1997: Journal of Volcanology and Geothermal Research, v. 93, p. 173–190.

Lahr, J.C., 1999, HYPOELLIPSE; a computer program for determining local earthquake hypocentral parameters, magnitude, and first motion pattern (Y2K compliant version): U.S. Geological Survey Open-File Report 99-23, 48 p.

Lalla, D.J., and Power, J.A., 2010, A two-step procedure for calculating earthquake hypocenters at Augustine Volcano, *in* Power, J.A., Coombs, M.L., and Freymueller, J.T., eds., The 2006 eruption of Augustine Volcano, Alaska: U.S. Geological Survey Professional Paper 1769 (this volume).

Main, I., 1987, A characteristic earthquake model of the seismicity preceding the eruption of Mount St. Helens on 18 May 1980: Physics of the Earth and Planetary Interiors, v. 49, p. 283–293.

McNutt, S.R., 2005, A review of volcanic seismology: Annual Review of Earth and Planetary Science, v. 33, p. 461–491, doi: 10.1146/annurev.earth.33.092209.122459.

Michael, A.J., 1987, Use of focal mechanisms to determine stress; a control study: Journal of Geophysical Research, v. 92, p. 357–368.

Mogi, K., 1962, Magnitude-Frequency relation for elastic shocks accompanying fractures of various materials and some related problems in earthquakes (2nd paper): Bulletin Earthquake Research Institute, v. 40, p. 831–853.

Mogi, K., 1963, Some discussions on aftershocks, foreshocks and earthquake swarms, the fracture of a semi-infinite body caused by an inner stress origin and its relation to the earthquake phenomena (Third Paper): Bulletin of the Earthquake Research Institute-University of Tokyo, v. 41, p. 615–658.

Okada, Hm., Watanabe, H., Yamashita, H., and Yokoyama, I., 1981, Seismological significance of the 1977–1978 eruptions and the magma intrusion process of Usu volcano, Hokkaido: Journal of Volcanology and Geothermal Research, v. 9, p. 311–334.

Okada, Hm., 1983, Comparative study of earthquake swarms associated with major volcanic activities, *in* Shimozuru, D., and Yokoyama I., eds, Arc volcanism: physics and tectonics: Tokyo, TERRAPUB, p. 43–63.

Power, J.A., Nye, C.J., Coombs, M.L., Wessels, R.L., Cervelli, P.F., Dehn, J., Wallace, K.L., Freymueller, J.T., and Doukas, M.P., 2006, The reawakening of Alaska's Augustine Volcano: EOS (American Geophysical Union Transactions), v. 87, p. 373, 377.

Power, J.A., and Lalla, D.J., 2010, Seismic observations of Augustine Volcano, 1970–2007, *in* Power, J.A., Coombs, M.L., and Freymueller, J.T., eds., The 2006 eruption of Augustine Volcano, Alaska: U.S. Geological Survey Professional Paper 1769 (this volume).

Qamar, A., St. Lawrence, W., Moore, J.N., and Kendrick, G., 1983, Seismic signals preceding the explosive eruption of Mount St. Helens, Washington, on 18 May 1980: Bulletin of the Seismological Society of America, v. 73, p. 1797–1813.

Reasenberg, P., and Oppenheimer, D., 1985, FPFIT, FPPLOT, and FPPAGE; Fortran computer programs for calculating and displaying earthquake fault-plane solutions: U.S. Geological Survey Open-File Report 85-739, 25 p.

Robinson, M., 1990, XPICK users manual, version 2.7: Seismology Lab, Geophysical Institute, University of Alaska Fairbanks, 93 p.

Roman, D.C., Moran, S.C., Power, J.A., and Cashman, K.V., 2004, Temporal and spatial variation of local stress fields before and after the 1992 eruptions of Crater Peak vent, Mount Spurr Volcano, Alaska: Bulletin of the Seismological Society of America, v. 94, no. 6, p. 2366–2379.

Sanchez, J.J., McNutt, S.R., Power, J.A., and Wyss, M., 2004, Spatial variations In the frequency-magnitude distribution of earthquakes at Mount Pinatubo Volcano: Bulletin of the Seismological Society of America, v. 94, no. 2, p. 430–438.

Scholz, C.H., 1968, The frequency-magnitude relation of microfracturing in rock and its relation to earthquakes: Bulletin of the Seismological Society of America, v. 58, no. 1, p. 399–415.

Warren, N.W., and Latham, G.V., 1970, An experimental study of thermally induced microfracturing and its relation to volcanic seismicity: Journal of Geothermal Research, v. 75, no. 23, p. 4455–4464.

Wessels, R.L., Coombs, M.L., Schneider, D.J., Dehn, J., and Ramsey, M.S., 2010, High-resolution satellite and airborne thermal infrared imaging of the 2006 eruption of Augustine Volcano, *in* Power, J.A., Coombs, M.L., and Freymueller, J.T., eds., The 2006 eruption of Augustine Volcano, Alaska: U.S. Geological Survey Professional Paper 1769 (this volume).

Wiemer, S., 2001, A software package to analyze seismicity—ZMAP: Seismological Research Letters, v. 72, no. 2, p. 373–382.

Wiemer, S., and McNutt, S.R., 1997, Variations in the frequency-magnitude distribution with depth in two volcanic areas—Mount St. Helens, Washington, and Mt. Spurr, Alaska: Geophysical Research Letters, v. 24, no. 2, p. 189–192.

Wiemer, S., McNutt, S.R., and Wyss, M., 1998, Temporal and three-dimensional spatial analyses of the frequency-magnitude distribution near Long Valley Caldera, California: Geophysical Journal International, v. 134, p. 409–421.

Woessner, J., and Wiemer, S., 2005, Assessing the quality of earthquake catalogues; estimating the magnitude of completeness and its uncertainty: Bulletin of the Seismological Society of America, v. 95, no. 2, p. 684–698.

Wyss, M., 1973, Towards a physical understanding of the earthquake frequency distribution: Geophysical Journal of the Royal Astronomical Society, v. 31, p. 341–359.

Zobin, V., 1979, Variations of volcanic earthquake source parameters before volcanic eruptions: Journal of Volcanology and Geothermal Research, v. 6, p. 279–293.

Appendixes 1–2

Appendix 1. Start Date Algorithms

Algorithm Descriptions

Two algorithms were developed to quantitatively assign a start date for the Augustine 2005–6 preeruptive earthquake swarm. We call these algorithms the largest daily count method (LDCM), and the consecutive days method (CDM). Although the algorithms are written in a general format, they are tailored to Augustine Volcano. Each method requires a year of data to establish background rates. This period was chosen because earthquake rates at Augustine are generally steady for years at a time and the year–long period should eliminate any small seasonal or weather biases in the ability to locate earthquakes. Once the background rate has been established, we have a basis to look for increased rates of activity. Both algorithms assume that a swarm has already been detected; however, they could be run continuously on data with a moving background window to "search" for swarms. We use only located earthquakes in the algorithms; again, this is practical for Augustine, but isn't necessarily suitable for volcanoes where a large number of unlocated or long-period earthquakes occur. The CDM algorithm in particular is only suited to volcanoes with fairly low earthquake rates.

Both algorithms use the same initial background analysis to establish a trigger threshold for the selection of periods of increased activity or the occurrence of a swarm. We have chosen one–eighth of the total earthquakes from the previous year occurring in a period of 30 days as the trigger threshold for increased activity. The expected seismicity in an average 30-day period would be one–twelfth of the annual seismicity. Setting a threshold of one–eighth allows for monthly and seasonal variations within the yearly average, but also keeps the threshold low enough to detect small increases in rate. Later stages of the algorithms ensure that these initial triggers are not ordinary behavior. Once a trigger is found, another set of background calculations is performed on the 4 months prior to the beginning of the trigger to determine normal fluctuations in the earthquake rate.

The LDCM algorithm uses the daily number of located earthquakes. This is done by establishing another set of background criteria once a swarm is recognized. First the weekly average of the 4 months prior to the trigger is taken, and also the largest event count for a single day is found. These 4 months are then tested to see if there are any weeks within the 4 months that exceed three times the weekly average. If there is no week that exceeds three times the average in the 4 months, then the trigger period is searched for 7-day periods that exceed the weekly average. If a week is found within the trigger period that exceeds three times the weekly average, then the largest event count for that week is compared to the largest event count for the 4-month background. If there is a week that exceeds three times the weekly average of the previous 4 months and the highest daily event count in that week is equal to or exceeds the highest daily event count for the 4 months of background, then that day is taken as the swarm start date. Figure 17 is a flow chart diagram for the LDCM method.

Augustine Volcano has very low earthquake rates and many days without any located earthquakes. The CDM algorithm uses the number of consecutive days with located earthquakes as a second way to look for increased activity. Using the same initial trigger period as LDCM, we then define two more background parameters to search for the swarm start date. The first is the number of consecutive days with located earthquakes, and the second is the number of earthquakes found commonly within a short (1 to 5 days) span. For instance, at Augustine three earthquakes in 3 days is a common occurrence. The background period is analyzed to see how often this occurs and what the shortest time interval of reoccurrence is. Once this is established, the 30-day trigger period is searched for periods of time that meet the criteria of number of events in the shorter time frame. If the first instance found meets but does not exceed the number of earthquakes, then we look for another instance. If another instance is found, we look at the time interval between these instances and compare that to the occurrence information gathered from the background data. We continue searching for occurrences until one exceeds the thresholds of the background, or there are enough triggers in a short amount of time that we believe activity has increased, or activity returns to background for two weeks or more. Figure 18 is a flow chart diagram for the CDM method.

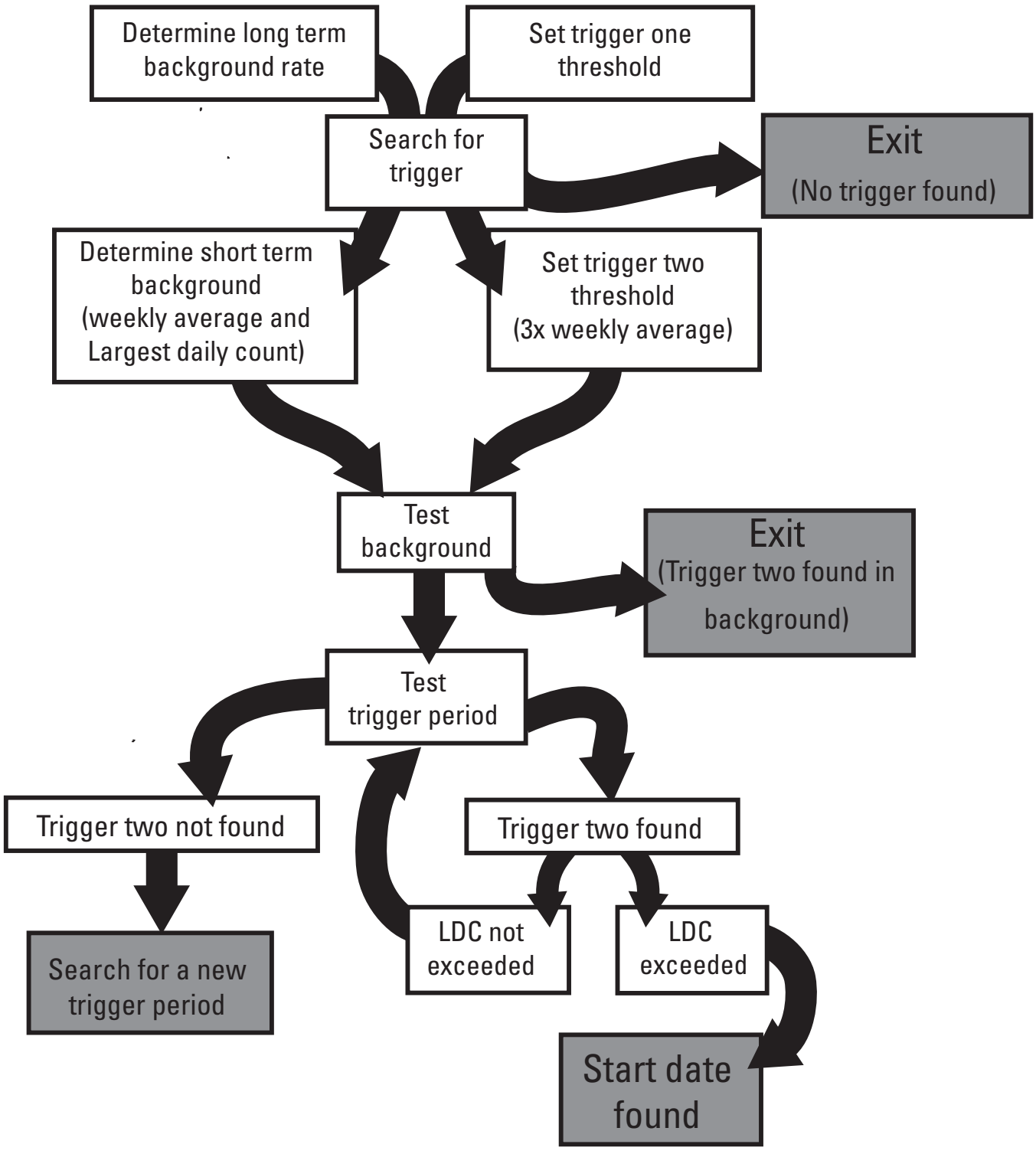

Figure 17. Flow–chart diagram illustrating the largest daily count method (LDCM) for swarm start–date determination.

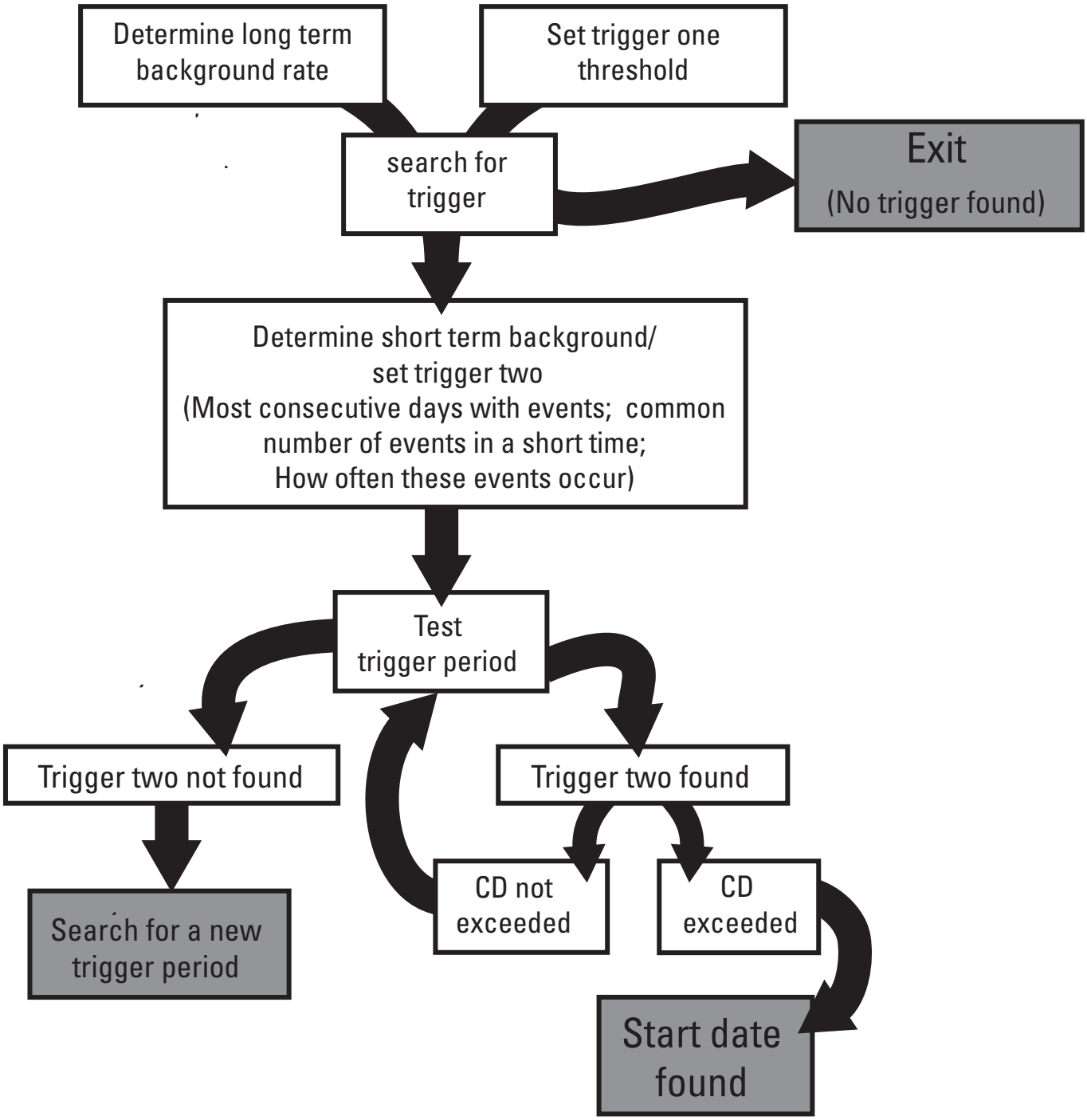

Figure 18. Flow–chart diagram illustrating the consecutive days method (CDM) for swarm start–date determination.

Results of LDCM and CDM Algorithms for the Augustine 2005–2006 Preeruptive Earthquake Swarm

Although the two algorithms use the same initial steps to classify earthquake activity as increased above background, they use unique secondary classifications to narrow down the start date. Both algorithms give a swarm start date of April 30, 2005. The detailed results for each step of the algorithms are given below.

Largest Daily Count Method

Define a reasonable background rate that is unbiased of previous swarms and annual weather phenomena:

- Calculate the previous calendar year's located earthquakes. Taking the average of an entire year's worth of data should eliminate most seasonal weather affects.
  Augustine: 238 located earthquakes total in 2004

Define a trigger to look for a swarm start date:

- Search for a 30-day period that exceeds 12.5 percent (1/8) of last year's earthquake total. Augustine: 238÷8 = 30 earthquakes
  Augustine: 4/14/2005–5/12/2005 = 31 earthquakes

If a trigger occurs, calculate the following data in order to define and test what is now taken to be the background seismicity rate:

- Take the weekly average for the 4 months prior to the 30 days of data in the trigger.
  Augustine: Two earthquakes per week
- Find the largest event count for a single day in those four months.
  Augustine: Three earthquakes in a single day

Test the background data calculated to see how representative the average daily located earthquake count is of the data:

- Search for weeks within the 4–month background period that exceed three times the weekly average calculated.
  Augustine: None
- If no week within the background period exceeds three times the weekly average of that period, then search for the first week in the 30-day trigger period that exceeds three times the background weekly average.
- If the weekly average and largest daily located earthquake counts are found to be unrepresentative of the time period, another method or calculation may be necessary.

Search the trigger period for deviations from the background averages:

- Search for the first week within the 30-day trigger period that exceeds three times the background weekly average.
  - If a week within the trigger period meets this criterion, find the largest daily earthquake count in that week.
    Augustine: Week of April 14th, six earthquakes, two in one day
- Compare this daily earthquake count to the largest daily earthquake count for the background period.
  - If the daily earthquake count for the trigger period week is less than the largest daily earthquake count for the background period, continue searching for another week that exceeds three times the weekly average and repeat as necessary.
    Augustine: Week of April 28th, nine earthquakes, five in one day
  - If the largest daily earthquake count for the trigger period is greater than or equal to the largest daily earthquake count for the background period, select that date as the start date.
    Augustine: Week of April 28th, nine earthquakes, five in one day (April 30th)
    Start Date: April 30th

Consecutive Days Method

Define a reasonable background rate that is unbiased of previous swarms and annual weather phenomena:

- Calculate the previous calendar year's located earthquakes. Taking the average of an entire year's worth of data should eliminate most seasonal weather affects.
  Augustine: 238 located earthquakes total in 2004

Define a trigger to look for a swarm start date:

- Search for a 30-day period that exceeds 12.5 percent (1/8) of last year's earthquake total.
  Augustine: 238÷8 = 30 earthquakes.Augustine: 4/14/2005-5/12/2005 = 31 earthquakes

If a trigger occurs, calculate the following data in order to define and test what is now taken to be the background seismicity rate:

- Define normal rates of continuous seismicity.
  - What is the longest string of consecutive days during normal activity?
    Augustine: 3 days
  - Find a value of consecutive days that is high, but occurs more than once.
    Augustine: 3 days (this is the longest string and occurs several times)
- Define normal numbers of earthquakes during the continuous seismicity.
  - Tally the highest number of events during these times.
    Augustine: Three earthquakes (in 3 days)
  - How often does this occur?
    Augustine: An average of every 13 days
  - What is the shortest time interval between occurrences?
    Augustine: One day (ranges to 30 days)

Search the trigger period for deviations from the background averages:

If there is a string of days that meets the consecutive day threshold or the events within a time threshold, look for a swarm.

- How many earthquakes are there?
- How does this compare to the normal number of earthquakes in a continuous period?
  Augustine triggers:
  April 14th: Three earthquakes, 3 days,
  Meets threshold
  April 18th: Three earthquakes, 2 days,
  Meets threshold
  ***April 24th: Three earthquakes, 1 day,**
  Meets threshold
  April 30th: Five earthquakes, 1 day,
  Exceeds threshold
  ***This is the shortest time between any three triggers in the background**
- Once a trigger is found that exceeds the threshold, this day (or the beginning of the set) is the swarm start date.

Start Date: April 30th

Appendix 2. Focal Mechanisms

Focal mechanisms were computed for all earthquakes using FPFIT (Reasenberg and Oppenheimer, 1985). Solutions were judged acceptable if they had: a misfit of less than 0.15 (less than 15 percent of stations inconsistent with the preferred solutions), STDR (distribution around the hypocenter) ≥ 0.40, and an average uncertainty in strike, dip, and rake of ≤ 25º. Below are 79 (out of 201) earthquakes that returned acceptable focal mechanisms. There were 19 events (out of 61 picked) with acceptable solutions from 2002 through 2004, and 60 events (out of 140 picked) from the long swarm (all events with acceptable solutions in 2005 occurred during the long swarm). If FPFIT returned two or more solutions for the same earthquake, we have retained the solution with the lowest combination of errors. Mechanisms are arranged with time starting from 2002 and getting later down each column and across each page.

Fault-plane solutions for 79 earthquakes occurring at Augustine volcano from May 24, 2002 to January 6, 2006. P, compressional axis; T, tensional axis. Open circles correspond to dilatational (down) first motions, crosses to compressional (up) first motions. Each solution is coded for date and time (UTC) in this format: YYYYMMDD hhmm. Z, depth, in kilometers; *M*, magnitude.

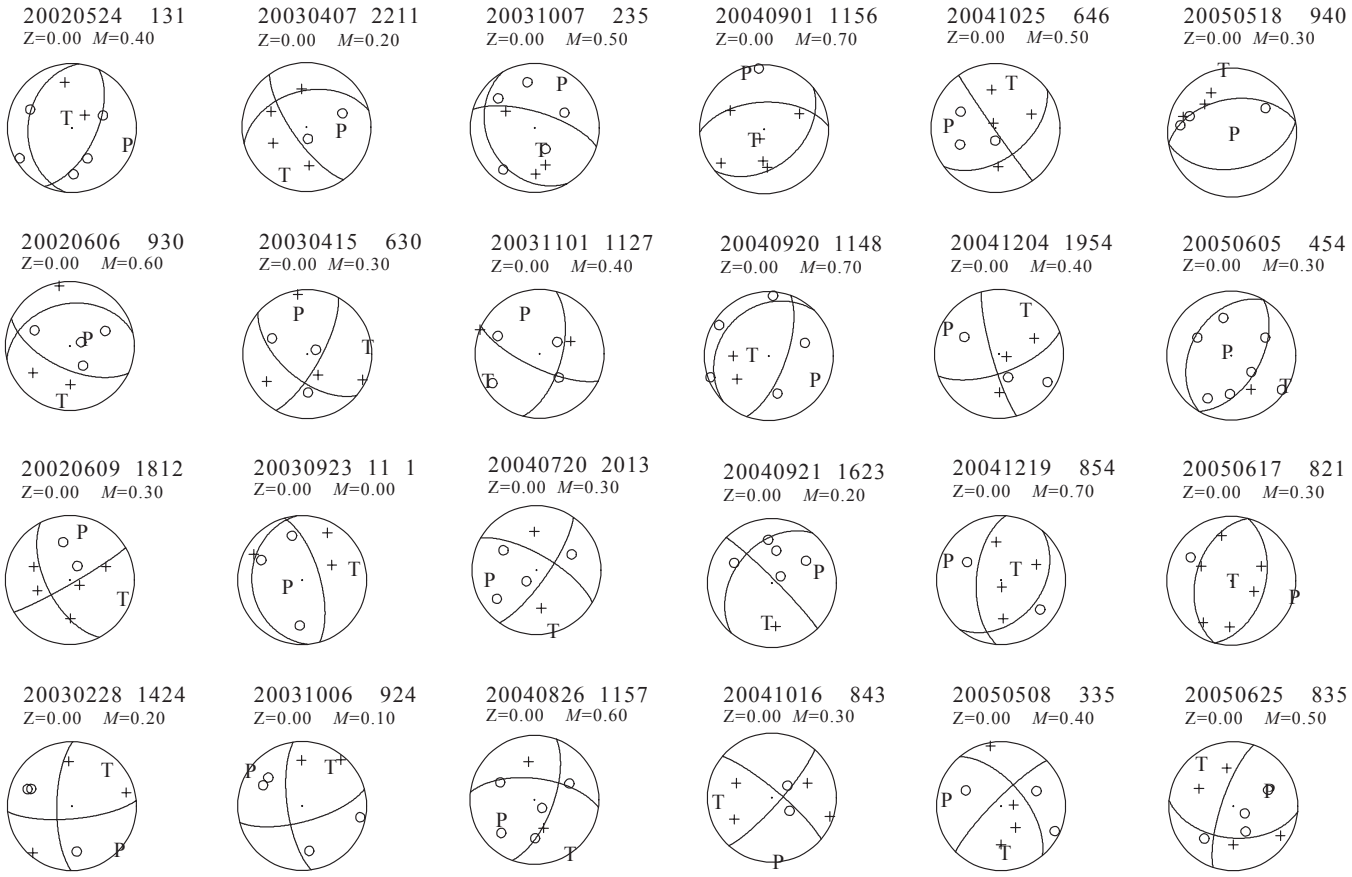

20050811 1732
Z=0.00 *M*=0.30

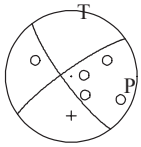

20051005 1329
Z=0.00 *M*=0.60

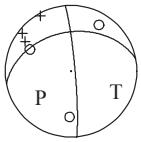

20051130 1047
Z=0.00 *M*=0.40

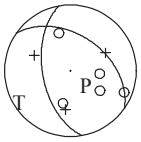

20051211 2358
Z=0.00 *M*=0.50

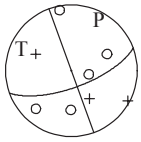

20051219 1126
Z=0.00 *M*=0.40

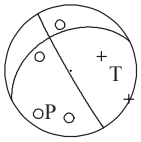

20051224 251
Z=0.00 *M*=1.10

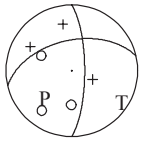

20050828 931
Z=0.00 *M*=0.30

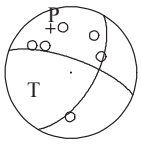

20051030 1939
Z=0.00 *M*=0.40

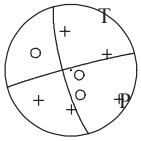

20051130 1639
Z=0.00 *M*=0.30

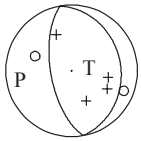

20051215 5 4
Z=0.00 *M*=0.80

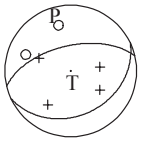

20051221 323
Z=0.00 *M*=0.80

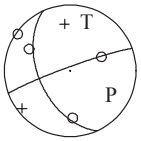

20051224 817
Z= 0.00 *M*=0.60

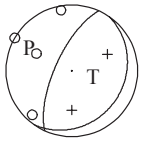

20050919 2046
Z=0.00 *M*=0.60

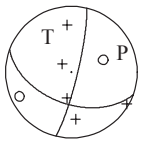

20051115 1740
Z=0.00 *M*=0.40

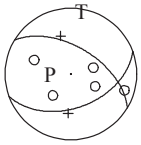

20051202 920
Z=0.00 *M*=0.70

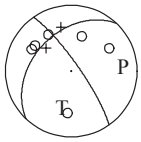

20051217 637
Z=0.00 *M*=0.60

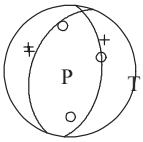

20051221 446
Z=0.00 *M*=0.70

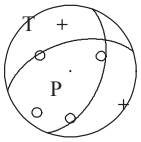

20051224 9 8
Z= 0.00 *M*=0.80

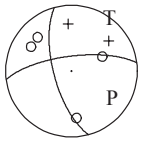

20050919 2051
Z=0.00 *M*=0.90

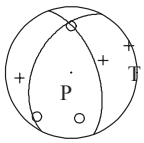

20051127 1821
Z=0.00 *M*=0.40

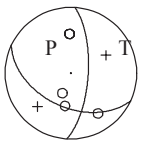

20051208 053
Z= 0.00 *M*=0.50

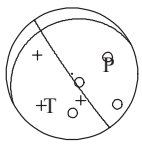

20051217 1149
Z=0.00 *M*=0.30

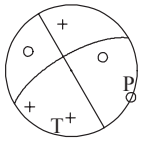

20051221 16 5
Z=0.00 *M*=0.60

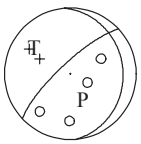

20051222 2241
Z=0.00 *M*=0.60

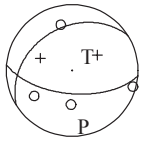

20051004 124
Z=0.00 *M*=0.30

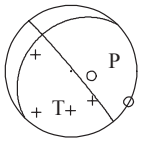

20051129 1641
Z=0.00 *M*=0.30

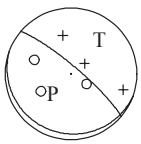

20051211 2222
Z= 0.00 *M*=0.40

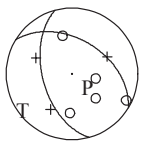

20051219 10 1
Z=0.00 *M*=1.00

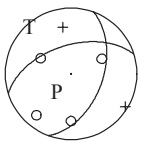

20051224 227
Z=0.00 *M*=0.60

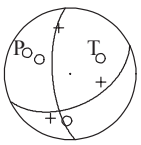

20051222 2242
Z=0.00 *M*=0.80

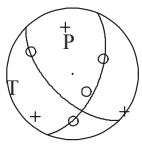

Continued.

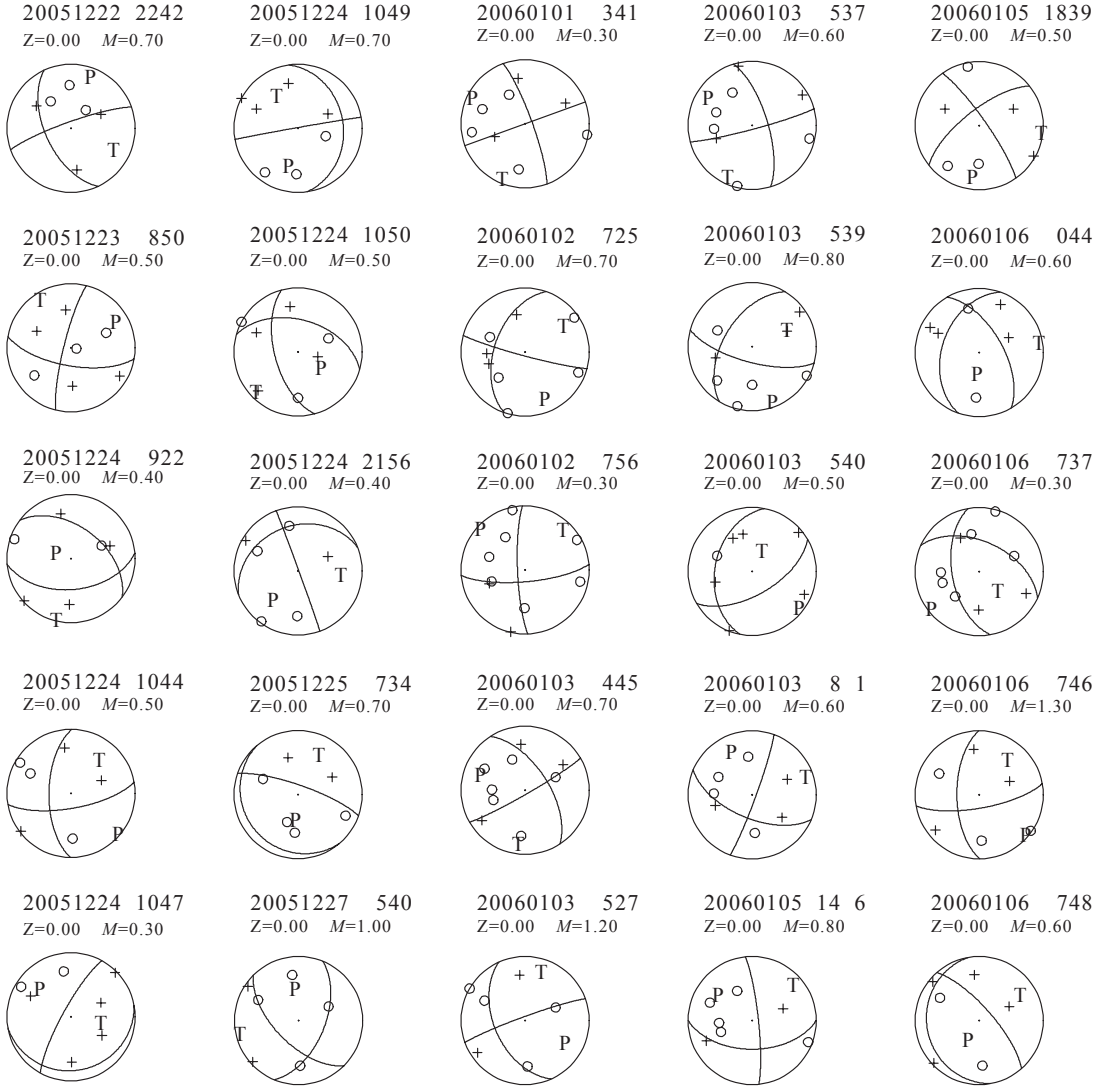
20051222 2242
Z=0.00 M=0.70
20051224 1049
Z=0.00 M=0.70
20060101 341
Z=0.00 M=0.30
20060103 537
Z=0.00 M=0.60
20060105 1839
Z=0.00 M=0.50
20051223 850
Z=0.00 M=0.50
20051224 1050
Z=0.00 M=0.50
20060102 725
Z=0.00 M=0.70
20060103 539
Z=0.00 M=0.80
20060106 044
Z=0.00 M=0.60
20051224 922
Z=0.00 M=0.40
20051224 2156
Z=0.00 M=0.40
20060102 756
Z=0.00 M=0.30
20060103 540
Z=0.00 M=0.50
20060106 737
Z=0.00 M=0.30
20051224 1044
Z=0.00 M=0.50
20051225 734
Z=0.00 M=0.70
20060103 445
Z=0.00 M=0.70
20060103 8 1
Z=0.00 M=0.60
20060106 746
Z=0.00 M=1.30
20051224 1047
Z=0.00 M=0.30
20051227 540
Z=0.00 M=1.00
20060103 527
Z=0.00 M=1.20
20060105 14 6
Z=0.00 M=0.80
20060106 748
Z=0.00 M=0.60

Continued.